Bulletin of Volcanology

Magnetotelluric imaging of the resurgent caldera on the island of Ischia (Southern Italy): inferences for its structure and activity

--Manuscript Draft--

Manuscript Number:	BUVO-D-17-00072R4
Full Title:	Magnetotelluric imaging of the resurgent caldera on the island of Ischia (Southern Italy): inferences for its structure and activity
Article Type:	Research Article
Corresponding Author:	Stefano Carlino Istituto Nazionale di Geofisica e Vulcanologia Sezione di Napoli ITALY
Corresponding Author Secondary Information:	
Order of Authors:	Maria Giulia Di Giuseppe
	Antonio Troiano
	Stefano Carlino
Funding Information:	
Abstract:	The island of Ischia (located in the Bay of Naples, Italy) represents a peculiar case of a well-exposed caldera that has experienced a large (>800 m) and rapid resurgence, accompanied by volcanic activity. What drives the resurgence of calderas is a crucial issue to investigate, because this process is associated with potential eruptions and high risk to people living within and around such large active volcanic systems. To improve the knowledge of volcano-tectonic processes affecting the caldera of Ischia electromagnetic imaging of the structures associated with its resurgence was performed and integrated with available geological information. A magnetotelluric (MT) survey of the island was carried out along two main profiles through the central-western sector, providing an electrical resistivity map to a depth of 3 km. These resistivity cross-sections allowed us to identify the presence of a very shallow magmatic intrusion, possibly a laccolith, at a depth of about 1 km, which was responsible for both the resurgence and the volcanic activity. Furthermore, the tectonic structures bordering the resurgent area and the occurrence of a large thermal anomaly in the western sector of the caldera also provided a signature in the resistivity cross-sections, with the magma intrusion producing advection of hot fluids with high geothermal gradients (>150 °C km-1) in the southern and western sectors. All of these data are fundamental for the assessment of the island's volcano-tectonic dynamics and their associated hazards. The structure and activity of the island have been controlled by the process of resurgence associated with the arrival of new magma and the progressive intrusion of a laccolith at a shallow depth. The reactivation of such a shallow system may imply imminent eruption which would pose a major volcanic hazard.
Response to Reviewers:	Dear Editor We would like to thank you for your further revision that greatly improved the quality of the work. All your corrections and comments have been reported and followed in the new text. Figure and captions have also been changed. You can find all the changes in the tracking copy of the paper. We cannot reported the vertical scale in the figure 8 because it is difficult to read due to the points of view. We avoid this problem reporting the height of the Mt. Epomeo. Regards
Author Comments:	In this work we provide new data about the active volcanic island of Ischia (Gulf of Naples, Italy) inferred from a geophysical survey. In particular, a magnetotelluric survey of the island has been performed along two main profiles of the central-western sector, obtaining the first electrical resistivity map down to a depth of 3km. The island undergone to a resurgence process, of at least 800m, forming a central uplifted block around which explosive and effusive volcanic activity occurred during the last 55ka (last eruption occurred in 1302). The island is still active and is characterized by a large

	hydrothermal system with high heat flow and geothermal gradient up to 250°Ckm-1. The presence of a stable population of about 65.000 units, and more than 1.500.000 visitors during the spring-summer season, makes the volcanic risk of this area very high. The volcano dynamic of the island is thus necessarily to be evaluated, firstly by improving the knowledge of shallow and deep geology of the island. The interpretation of resistivity variations allow us to recognize the main volcano-tectonic features of central-western part of the island, along the two profiles, such as the presence of a possible very shallow magmatic intrusion to a depth of about 1km, the tectonic structures bordering the resurgent area and the occurrence of large thermal anomaly of the western sector. All these data are fundamental for the assessment of volcano-dynamic of the island and associated risk.

Magnetotelluric imaging of the resurgent caldera on the island of Ischia (Southern Italy): inferences for its structure and activity

Di Giuseppe, M. G., Troiano, A. and *Carlino, S.

Istituto Nazionale di Geofisica e Vulcanologia, Sezione di Napoli – Osservatorio Vesuviano (Italy)
*Corresponding author: stefano.carlino@ingv.it

Abstract

The island of Ischia (located in the Bay of Naples, Italy) represents a peculiar case of a well-exposed caldera that has experienced a large (>800 m) and rapid resurgence, accompanied by volcanic activity. What drives the resurgence of calderas is a crucial issue to investigate, because this process is associated with potential eruptions and high risk to people living within and around such large active volcanic systems. To improve the knowledge of volcano-tectonic processes affecting the caldera of Ischia electromagnetic imaging of the structures associated with its resurgence was performed and integrated with available geological information. A magnetotelluric (MT) survey of the island was carried out along two main profiles through the central-western sector, providing an electrical resistivity map to a depth of 3 km. These resistivity cross-sections allowed us to identify the presence of a very shallow magmatic intrusion, possibly a laccolith, at a depth of about 1 km, which was responsible for both the resurgence and the volcanic activity. Furthermore, the tectonic structures bordering the resurgent area and the occurrence of a large thermal anomaly in the western sector of the caldera also provided a signature in the resistivity cross-sections, with the magma intrusion producing advection of hot fluids with high geothermal gradients (>150 °C km^{-1}) in the southern and western sectors. All of these data are fundamental for the assessment of the island's volcano-tectonic dynamics and their associated hazards. The structure and activity of the island have been controlled by the process of resurgence associated with the arrival of new magma and the progressive intrusion of a laccolith at a shallow depth. The reactivation of such a shallow system may imply imminent eruption which would pose a major volcanic hazard.

Introduction

The resurgence of calderas was defined by Smith and Bailey (1969) as the process of uplift that usually occurs in the form of a structural dome that takes place after a caldera collapse. The uplift and bending of both the floor and roof of the caldera produce fracturing, faulting and, thereby, enhance the development of permeability channels (Kennedy *et al.*, 2012). While generation of highly permeable network promotes the circulation of hot fluids, forming magmatic-hydrothermal systems (Hulen *et al*, 1987), faulting and fracturing can also facilitate the migration of magma to the surface and, eventually, an eruption (Kilburn, 2003). Thus, resurgence plays a central role in the evolution of calderas, but the processes involved are still unclear, in particular with regard to the causes and the timing of uplift. The most common process associated with the resurgence of calderas is the influx or intrusion of magma at various depths (Fridrich *et al*., 1991; Saunders, 2001; Jellinek and De Paolo, 2003; Kawakami *et al*., 2007). Other mechanisms contributing to resurgence have been suggested, such as combination of regional detumescence and viscous rebound (Smith and Bailey, 1969; Marsh, 1984), volatile exolution and gas overpressure (Marsh, 1984), thermal expansion of the caldera fill (Kennedy and Stix, 2003) and the disturbance of geothermal fluids (Hurwitz *et al*., 2007; Chang *et al*., 2010, Troiano *et al*., 2011).

A crucial question is thus, what drives resurgence within calderas and (if magma is involved in this process), at what depths and of what volumes are the resultant intrusions? In the latter case, depending on the volcano-tectonic setting, the rate of uplift of the area and magma viscosity (Pollard and Johnson,1973; Smith and Bailey, 1969; Acocella *et al*., 2001; Carlino, 2012), the magmatic intrusion may evolve in a range of ways (e.g. to be emplaced as sills, dikes or laccoliths) producing a variable amount of uplift and a variety of resurgence structures (Paige, 1913; Orsi et al., 1991; Henry *et al*., 1997; Acocella *et al*., 2001 and references therein). The recognition of such differences is fundamental in the understanding a caldera structure and any associated hazard. As a result the shallow and deep structures of calderas need to be better investigated through the application of effective geophysical methods. Among the geophysical surveys that can improve the knowledge of the deep structures of calderas, electrical resistivity mapping represents a reliable tool in the assessment of the buried structures in volcanic settings (Troiano *et al*., 2008; Troiano *et al*., 2009; Revil *et al*., 2010; Troiano *et al*., 2014; Di Giuseppe *et al*., 2015; Di Giuseppe *et al*., 2017b).

In this work, a magnetotelluric (MT) survey was applied to the active volcanic caldera of Ischia, whose resurgence is thought to be associated to a sill intrusion, possibly developed in the form of a laccolith (Rittman, 1930; Sbrana *et al*., 2009; Carlino *et al*., 2006; Carlino, 2012 and references therein). The resurgence, which is estimated as at least 800 m (Vezzoli, 1988), was accompanied by volcanic activity and by the exhumation of the geothermal system (Sbrana et al., 2009), with the occurrence of a large diffuse heat flow and very high geothermal gradients (>180°C km^{-1}) in the shallow crust (Vezzoli, 1988; Carlino, 2012; Carlino *et al*., 2014; Carlino *et al*., 2015). Although a numbers of local geophysical investigations have been performed at Ischia (Di Napoli *et al*., 2009, 2011; Paoletti *et al*., 2013), a wider geophysical imaging of the island is not yet available. Such knowledge represents a crucial task in supporting physical modeling (Rinaldi et al., 2011), to improve the understanding of the caldera's structure and activity, and to assess the associated hazard on the island.

The MT survey was carried out in the central-western sector of the island. Through this survey, the electrical resistivity distribution was reconstructed in correspondence to two separate profiles (deployed in a N-S and a WSW-ENE direction respectively) (Figure 1). In this fashion two resistivity sections, respectively about 5 km and 3 km long, were obtained and interpreted to highlight the main geological features of the crust to a depth of 3 km including its thermal state, as well as location of fluid circulations and structural discontinuities within both the collapsed and the uplifted areas. The results provide new insights regarding both the thermal situation pertaining on the central-western sector of the island and the circulation of geothermal fluids. We find presence of a crystalline structure (intrusive rocks with very low permeability) located beneath the Mount Epomeo block (Figure 1), which possibly represents the apical part of a degassed and cooling magmatic source (laccolith). The results obtained are important, not only because of the volcanic risk on the island (which has about 65,000 inhabitants and more than 1,500,000 visitors during the spring and summer months) but also for the volcano-tectonic evolution observed in many calderas worldwide, during resurgence.

Main geological features of the island

The volcanic field of Ischia is part of the Phlegrean Volcanic District(Figure 1). The rim of Ischia caldera, which formed after the Mount Epomeo Green Tuff (MEGT) eruption, 55 ka (Vezzoli, 1988), is not well documented, although there are a few signs of the rim in the NW, SW and SE sectors (Tibaldi and Vezzoli, 1998). The caldera, it would seem, has an elliptical shape with its major axis running ENE-WSW (Vezzoli, 1988). The island's most important structural element is the 4x4 km^2 resurgent block of Mount Epomeo (formed mainly by the MEGT), located in the centre of the caldera, which has been uplifted over the last 55 ka by a magmatic intrusion (Rittman, 1930; Sbrana *et al*., 2009). The edges of this block are marked by a system of sub-vertical faults with NW-SE, NE-SW and N-S strike (Vezzoli, 1988; Acocella and Funiciello, 1999; Tibaldi and Vezzoli, 1998) (Figure 1). The existence of a possible magmatic intrusion, associated with the resurgence and post-caldera volcanic activity, was first inferred from gravity surveys by Carrara *et al*., (1983) and Nunziata and Rapolla (1987). More recently, the model of laccolith intrusion (proposed by Rittman, 1930) has been taken up again by interpreting stratigraphy, deep temperature, geochemical, magnetic, electric and gravity data (Carlino *et al*., 2006; Sbrana *et al*., 2009; Carlino 2012; Paoletti *et al*., 2013). Sbrana *et al*. (2009) provided a model of resurgence of the island by using an integrated analysis of melt and fluid inclusions, mineralogy and stable isotopic compositions of pumices, tuffs and syenitic xenoliths. In this model the engine of the hydrothermal system of Ischia can be identified as being a shallow magmatic system (at a depth of 2 km) that hosts hot trachytic magma. Accordingly, Carlino *et al*., (2006) and Carlino (2012) showed, through analytical modeling of the bending and fracturing of an elastic plate, that the resurgence of Mount Epomeo block may be associated to a sill-like intrusion which developed, during its later stages, into a laccolith, the top of which is located at a depth of about 2 km. Paoletti *et al*. (2013), using an integrated analysis of geophysical data, highlighted the presence of a possible magmatic intrusion, with a temperature below the Curie point, a density of about 2.4 g cm^{-3} and its top at a depth of about 2 km. The top of this magma body is slightly off-center, being in the southwestern part of Ischia where fumaroles emissions are focused (Chiodini et al., 2004). The total estimated uplift of the Mount Epomeo block, deduced from the present height of marine deposits and eustatic variations, is 710 m in the southern sector and 920–970 m in the northern sector, with average rate of uplift ranging from 2.3 to 3.3 cm a^{-1} (Barra *et al*. 1992; Tibaldi and Vezzoli 2004; Carlino *et al*. 2006). During the resurgence over the last 28 ka, most of the eruptive centres have been aligned along the caldera structure (Vezzoli, 1988). Between 28 ka and 18 ka the volcanic activity migrated to the SW and SE sectors of the island (Fusi et al., 1990). However, during the most recent period of activity, from 10 ka to 1302 A.D., the eruptive centers have become clustered in the eastern and northern sector, with the emission of domes and lava flows (de Vita *et al*., 2010). The last eruption in the island took place in 1302 A.D. (de Vita et al., 2010)

The circulation of hydrothermal fluids on the island is linked to its volcano-tectonic structural setting, whose permeability is controlled by the relative location of lavas and pyroclastic deposits. Fluid circulation is thus correlated with the occurrence and interlayering of different deposits, and mostly takes place at pathways of high permeability such as at fractures and faults in welded tuffs and lavas and within the pores of unconsolidated pyroclastic deposits (Celico *et al*., 1999; Carlino *et al*., 2014). The shallow stratigraphy of the western sector (down to a depth of 1 km) has been inferred from borehole measurements (Penta and Conforto, 1951; see figure 1 for borehole locations). In the central zone of Mt. Epomeo and along its boundary while coarse volcanic deposits form a shallow permeable layer, fractured tuffs, lavas and marine clay deposits make up semi-permeable and impermeable layers, respectively. In the western area of the island the aquifer generally has a lower transmissivity than in the eastern sector (Celico *et al*., 1999). The effect of volcano-tectonic structures is noticeable above the main faults bordering Mt. Epomeo, where the shallow aquifers have been pushed upward in correspondence to the uplift of the block (Sbrana *et al*., 2009; Carlino *et al*., 2014). Along the western faults hot springs are located about highly permeable path ways associated with high thermal energies (Chiodini *et al*., 2004) (Figure 1). Also inferred in the western sector is the occurrence of mixing processes between marine water and hydrothermal fluids, testified to by the high salinity of the fluids sampled close to the coast (Celico *et al*., 1999; Di Napoli *et al*., 2011). In the southwestern sector of the island the shallow resistivity model obtained by Di Napoli *et al*. (2011) highlights the presence of a zone of high conductivity, whose top is located at a depth of about 100 m and which is related to the superficial hydrothermal reservoir. Geothermal gradients of the island are typically very high, ranging in the hottest areas (south-western sector) from 180 °C km^{-1} to 200 °C km^{-1} (AGIP, 1987). These high gradients are associated with an efficient heat transport from the reservoir through an advection-dominated system (Carlino *et al*., 2012; Carlino *et al*., 2014). Taking into account these gradients, the transition from a brittle to semi-brittle regime should take place at a depth of about 2-3 km (Carlino *et al*., 2014), while the depth of the brittle crust is possibly deeper in the north with respect to the southern sector (Carlino *et al*., 2006). At present time the island is subject to slow subsidence, reflecting a gradual depressurization of the magmatic or hydrothermal system beneath Mount Epomeo (Sepe *et al*., 2007; De Martino *et al*., 2011).

MT data collection, analysis and inversion.

To characterize the first few kilometers of the crust of the island of Ischia a magnetotelluric survey was performed. Magnetotellurics is an electromagnetic geophysical method for measuring the resistivity of the earth's interior by recording the natural electric (**E**) and magnetic (**H**) fields on the surface (Vozoff, 1991) as they vary over tme. In the present application, fluctuations of the orthogonal components of these fields were recorded at 20 measurement sites (see figure 1 for locations). Measurements were carried out using a Stratagem EH4 instrument, produced by Geometrics. Only the horizontal components of the **E** and **H** fields were recorded, neglecting the sampling of Hz which is usually considered as only providing limited additional information regarding the dimensionality of the Earth's local structure (Vozoff, 1991; Simpson and Bahr, 2005). Once data set of field fluctuations over time had been collected, the underground resistivity complexity was obtained as a rank-2 tensor, **Z**, correlating the two orthogonal pairs (E_x, E_y) and (H_x, H_y) at the Earth's surface in the frequency-domain. This tensor is correlated with the MT apparent resistivity and phase curves, which compose the final dataset. To estimate such curves, the collected time series spectra have been estimated using a short period Fourier transform performed over the $10^{-4} \sim 10^{1}$ s range. Such a period was examined to investigate the structures located across the first few kilometers of depth below ground level. The investigated depth of the electromagnetic waves depends on their capacity to penetrate into the Earth. This, in turn, is directly related to rock resistivity. In a uniform substrate the electric and magnetic fields weaken exponentially with depth, the more conductive the rock, the lower the penetration. The depth at which the fields decline to e^{-1} of their values at the surface is termed the skin depth $\delta = (2\rho/\omega\mu)^{1/2} \approx 500(\rho/f)^{1/2}$ (in meters) where, ρ is the resistivity, f is the frequency of the wave, $\omega = 2\pi f$ and μ is the permeability. The latter is usually taken as being equal to μ_0 (free space permeability), except in highly magnetic materials. Frequency enters into the equations because the magnitudes of the induced telluric currents depend on the rate of change of the magnetic fields over time (Vozoff, 1991, Simpson and Bahr, 2005).

After the application of short period Fourier transform, data belonging to each of the MT surveys were analyzed using the algorithm of Egbert and Booker (1986). This was used to avoid the distortion in the estimated MT curves, which might emerge from the time series due to the presence of anthropic noise, especially for surveys in urban environments. This kind of algorithm has proven to be effective in the case of single station MT surveying (Egbert and Livelybrooks, 1996; Bai *et al.*, 2001; Brasse *et al.*, 2001; Pous *et al.*, 2002). Its application in such a context was tested during the electromagnetic imaging of the nearby Campi Flegrei area (Troiano *et al.*, 2014; Di Giuseppe *et al.*, 2017a) to analyze MT soundings. Its performance also proved to be adequate in the case of Ischia and the MT curves obtained do not appear affected by anomalous behavior, such as a strong scattering of the points, strong oscillations or rises in the apparent resistivity, etc., that might signal the presence of coherent noise. Finally, the MT curves were analyzed using both MT-corrector® and Winglink® commercial software (Figure 2).

One of the first issues concerning magnetotelluric data is the *static-shift* (Jones, 1988). The data may suffer a sort of indetermination in the level of the apparent resistivity curves, due to the galvanic effects of shallower bodies. Such an issue, that does not affect the phase curves, was taken into account by carrying out Local Electrical Resistivity Tomographies (ERT). ERT, being based on a DC current source, does not suffer such issues and it is possible to use tomography of this kind to synthetically reconstruct the correct level of the MT apparent resistivity at high frequency. Two separate profile lines, which were oriented along N-S and the WSW-WNE transects were set up. These profiles, 5 km and 3 km long respectively, covered the central-western sector of the island (figure 1). For each of the two profiles the apparent resistivity and phase curves relative to both the TM (Transverse magnetic) and TE (Transverse electric) modes are shown in figure 3, under pseudosection form (Vozoff, 1991).

As an initial step, the MT data dimensionality was analyzed. The introduced **Z**, which correlates the electric and magnetic fields on the Earth surface, presents peculiar characteristics in the case of 1D or 2D symmetries actually present in the data (Vozoff, 1991; Simpson and Bahr, 2005; Troiano *et al.*, 2009) and several approaches exist in the literature to investigate this issue, namely the Wal method (Weaver *et al*., 2000), phase tensor analysis method (Caldwell *et al*., 2004) and Groom and Bailey's method (McNeice and Jones, 2001).

In the present case, phase tensor analysis has been applied. This method, introduced by Caldwell *et al*. (2004) was well-described in Berdichevsky and Dmitrev (2010), where it is possible to retrieve details regarding the methodology, the definition of the phase tensor $[\Phi] = \begin{bmatrix} \Phi_{xx} & \Phi_{xy} \\ \Phi_{yx} & \Phi_{yy} \end{bmatrix}$ and all the derived quantities. Figure 4 reproduces the behavior of the orientation of the phase tensor ellipse, i.e. the $\alpha_1 = \frac{1}{2} sin\left(\frac{\Phi_{xy}+\Phi_{yx}}{\Phi_{xx}+\Phi_{yy}}\right)$ angle, defined in Berdichevsky and Dmitrev (2010); it is also reproduced the Caldwell-Bibby-Brown Skew angles, $skew_{CBB} = \frac{1}{2} arctan\left(\frac{\Phi_{xy}-\Phi_{yx}}{\Phi_{xx}+\Phi_{yy}}\right)$, for every survey, over four distinct frequency bands, respectively centered on 0.9, 9, 90 and 900 Hz. In a model with the two-dimensional regional background, $skew_{CBB} = 0$ and the principal directions of the phase tensor coincide with the α_1 angle. In the case of a 3D asymmetric regional background $skew_{CBB} \neq 0$. This angle represents a correction for the regional background asymmetry, which can be neglected if small, so that we can rely on the 2D approximation of the regional background. As expected in a volcanic context, the $skew_{CBB}$ does not seem to present a behavior adequate to support a 2D inversion and a different approach has to be pursued. It is worth noting that this step is the basis on which to choose one of the possible strategies that might prove to be more satisfactory for the data inversion.

Despite the well-tested 2D approach generally being thought of as the optimal to choose in terms of a compromise between the numerical complexities of the task and the affordability of the results, its incorrect application can lead to very misleading results and examples exist in literature where the differences originating from a 3D reinterpretation of previously analyzed MT data have led to models having very different implications (Booker, 2014). On the other hand, even if various 3D inversion codes have been proposed in the literature (Siripunvaraporn *et al*., 2005a; Kelbert *et al*., 2014) and if 3D inversion has been actually developed in MT surveying (Rosenkjaer *et al*., 2015; Yang *et al*., 2015), such a procedure is still not totally stable and requires a high number of sampling sites to be applied. In the Ischia survey work, the morphological conditions limited the number of sites and imposed the alignment of the sites along two crossed lines. This configuration has to be taken into account when the inversion strategy is questioned.

Many papers in the literature consider 3D inversion of 2D profiles (e.g. Ledo *et al*., 2002; Siripunvaraporn *et al*., 2005b). These highlight the limits of this approximation when the TM and TE apparent resistivity and phase are considered separately. Such a situation has also already been dealt with in Troiano *et al*. (2014), who presented a 3D inversion of an electromagnetic survey carried out in the Campi Flegrei area. In this case, the 1D inversion of the Z determinant has proved to be a useful tool to set up a strategy to interrogate the effects of buried structures in 3D based on 2D survey profiles. Such considerations prove to be particularly significant in volcanic environments (Ranganayaki, 1984; Pedersen and Engels, 2005; Troiano *et al*., 2014) and the resistivity model that can be obtained through this step, despite the strong limitation linked to the 1D approximation.

The likely indetermination related to the effects due to the eventual presence of lateral anomalies on the MT sections were here taken into account through a 3D based trial-and-error procedure (Troiano et al., 2014). The latter was carried out through the use of the subroutines of the WingLink® commercial code in order to estimate the apparent resistivity and phase curves. The subsoil was divided up into $76 \cdot 79 \cdot 36$ cells, with dimensions ranging from 50 m (in the core of the modeled area) up to 1 km (in the external zones) and an objective function was derived, based on the misfit between measured and reconstructed apparent resistivity and phases. This trial-and-error procedure begins with the resistivity model obtained using the 1D inversion of the Z determinant. A wide range of alternative models were then compared, taking as the most adequate that related to the lowest root mean square (r.m.s.). At the end of the procedure, an optimal model, corresponding to an r.m.s. less than seven, was selected. We note that the r.m.s. value obtained here was compatible with those presented for similar applications (e.g. Schwalenberg *et al*., 2002; Abdul Azeez and Harinarayana, 2007; Rao *et al*., 2007; Heise *et al*., 2008; Arango *et al*., 2009; Troiano *et al*., 2009 and Troiano *et al*., 2014).

An error threshold of 5% was considered for both the apparent resistivity and phase curves. More details for the data analysis and inversion procedures can be found in Troiano *et al*. (2008) and Troiano *et al*. (2014). The sections corresponding to the two profiles of figure 1 are represented in figure 5 and figure 6, respectively. The main electrical anomalies have been labeled with capital letters and will be interpreted geologically in the following section.

Considering a mean electrical resistivity for the medium of about 100 Ωm, the maximum period of 10 s was found to be associated with a wave penetrating more than 15 km into the crust. The models of figure 5 and figure 6 resolve to a maximum depth of about 3 km.. A full sensitivity analysis was also carried out, following Schwalenberg *et al*. (2002). In figure 7 the sensitivity maps are reported, relative to the resistivity cross-sections of both figures 5 and 6. Sensitivity represents an estimate of the changes induced in the data by infinitesimal variations in the underground electrical resistivity. There is no univocal threshold for the sensitivity required to indicate that a structure is well resolved, but the procedure presented in Troiano *et al*. (2008) and Troiano *et al*. (2009) supports the conclusion that both our resistivity cross-sections are reliable. The consistency of the main bodies retrieved in the sections was further questioned by removing the anomaly from the model and recalculating the relative r.m.s. Significant r.m.s. variations with respect to the error thresholds can be considered as an indicator that the investigated part of the model exhibits good resolution. For example, in the NS section of figure 5, the resolution of the zones labeled as A, B1, B2 and C was tested. When the resistivity of the model was modified only zone A, substituting the few tens of Ωm retrieved with the data inversion using the 200 Ωm identified in the surrounding area, a 13.4% change in the r.m.s. was obtained. This indicates that the A zone exhibits good resolution. Analogous results were obtained for all other zones.

Results

The resistivity imaging of the island of Ischia has allowed us to recognize a number of sectors, down to a depth of 2-3 km, with resistivity anomalies that are ascribable to distinctive processes and physical conditions of the hydrothermal system below the caldera. From the S-N profile (Figure 5), moving from south to north, it is possible to highlight a relatively high resistivity zone extending to station I6 (Ischia6) (this is zone A where resistivity values of thousands of Ωm). There is then a lower resistivity channel (zone B, with a few tens to hundreds of Ωm) between the measurement stations I7 and I8, and a high resistivity zone (C) beneath the Mt. Epomeo resurgent block (several thousands Ωm at a depth below 1000 m, between stations I5 and I13). A further zone of lower resistivity (zone D) occurs on the northern coast (<50 Ωm).

Along the WSW-ENE profile (figure 6) a rapid change in resistivity (from several thousands of Ωm to a few tens of Ωm) is observed to the WSW. Beyond the anomaly beneath Mt. Epomeo (C1, a few thousand Ωm), four other zones can characterized. The first one is a channel with lower resistivity between the stations I20 and I21 (E) which is well developed down to the bottom of the profile (at a depth of 2.5 km). Within the interior of this channel, two lower resistivity zones (a few tens Ωm) appear: the first one (E1) is located at shallower depths, up to 500 m below the surface, and the second one (E2) develops from a depth of about 1500 m to the bottom of the profile. Finally, a roughly circular shallow area (F) with very low relative resistivity (less than ten Ωm) can be identified ENE to station I18 (figure 6).

The agreement between the two resistivity cross-sections of figures 5 and 6 have been evaluated in figure 8, where a stereographic view of the retrieved anomalies is provided. In the area where the two profiles intersect our magnetotelluric imaging detects a coherent resistive structure in correspondence to the Mt. Epomeo resurgent block.

Interpretation of the resistivity cross-sections

The sensitivity of electrical resistivity to the presence of groundwater provides electrical and electromagnetic methods with a high detectability power for resolving buried structures. However, once the presence of the electrical resistivity anomalies have been inferred in volcanic settings, the interpretation of the geophysical imaging remains inherently difficult. Because the resistivity of rocks is generally affected by the water content, alteration (through their clay content and clay mineralogy), salinity of the pore water and temperature, the physical properties of porous rocks in geothermal and volcanic areas remain poorly known (e.g. Revil *et al*. 2002, Revil *et al*. 2017a and Revil *et al*. 2017b). Groundwater in volcanic settings flows within porous materials, which may undergo a greater or lesser degree of alteration. This alteration is due to a chemical weathering of the minerals by the hot hydrothermal fluids, including hydration-dissolution processes of the volcanic glass and the formation of aluminosilicates such as clays and zeolites (Schön, 2015). Hydroelectric coupling in these porous rocks is influenced by the presence of these aluminosilicate minerals due to their role in blocking the connected pore space. Electrical conductivity provides two contributions. The first is associated with conduction within the pore water. The second is termed surface conductivity and is associated with conduction in the electrical double layer coating the surface of grains (Berdichevsky and Dmitriev, 2010; Schön, 2015)). Both of these processes can bring about an increase in conductivity and, using only resistivity data, it is not easy to separate surface from bulk conductivities at a given pore water conductivity. In our case, a numbers of ambiguities in the interpretation of our data were reduced by correlating the resistivity anomalies with data provided from drilling (see figure 1 for locations), down to depth of 1150 m, and with previous geophysical and geochemical modeling of the island provided by Nunziata and Rapolla (1987), Chiodini et al. (2004), Paoletti et al. (2005), Di Napoli et al (2009), Di Napoli et al., (2011), Carlino (2012), Paoletti et al., (2013), Carlino et al. (2014).

The resistivity contrasts between zones A, B, C and D of N-S profile (Figure 5) present a good correlation with the known volcano-tectonic features of the island, such as the boundary of caldera and the Mount Epomeo resurgent block. In particular, the structural limit of the caldera is recognizable in the southern sector, close to the station I6. A normal fault, with a NW-SE strike affecting the south-western sector of the resurgent block (see figure 1 for fault location) (Vezzoli, 1988), coincides with the resistivity contrast between stations I5 and I8. In addition, north of station I4, the resistivity variation pattern can be interpreted as the occurrence of minor faults facilitating the block uplift in the period since 33 ka ago (Vezzoli *et al*., 2009). In the northern sector (figure 5) a low resistivity zone, which deepens to about 700-800 meters down, between the coast to the inner part of the island, is perhaps attributable to the interface between saline water and fresh water due to the latter's buoyancy.

Between measurement stations I7 and I8 a lower resistivity channel can be identified (B in figure 5). In particular, two major anomalies (B1 and B2) have been detected along this channel. The shallower one, B1, has a vertical extent of up to about 450 m b.s.l., while the deeper one, B2, develops from about 1100 m to 2500 m b.s.l. Following hydrothermal studies of the island (Di Napoli *et al*., 2009, 2011) and drilling data (Penta and Conforto, 1951; Penta, 1963; AGIP, 1987), we can interpret the resistivity anomalies B1 and B2 as two aquifers, the former with a temperature of about 150°C, and the latter with a temperature of 250 °C (Chiodini et al., 2004). These are formed by mixing of liquid and vapour (Chiodini et al., 2004). The lower levels of the aquifer B1 and the upper level of the aquifer B2 are in good agreement with the hydrothermal model proposed by Di Napoli *et al*. (2011). Along the WSW-ENE profile (Figure 6) two zones, E1 and E2, have been interpreted as two aquifers similar to those inferred along the N-S profile (B1 and B2). In accordance with the vertical tectonic movement of the island (resurgence), the top of aquifer B2 (N-S profile of figure 5) is closer to the uplift block and has been dislocated upwards with respect to the aquifer E2. The bottom of the aquifers are possibly sealed by argillfication processes which took place before resurgence. Furthermore, as shown in Figure 9, the shape and location of the whole channel exhibiting low resistivity is possibly reconcilable with a thermal anomaly (a plume) associated with advection of hydrothermal fluids. This is an interpretation also supported by drill hole data and by the presence of fumaroles and a hot-spring field (with temperatures up to 100°C), immediately north and west of stations I20 and I21, respectively (Citara site, figure 1) (Penta and Conforto, 1951; AGIP, 1987; Chiodini *et al*., 2004; Di Napoli *et al*., 2011; Carlino *et al*., 2014). The presence of such a thermal plume should leave a clear geophysical signature and the futher surveys might allow it to be fully characterized (Jardani *et al*., 2008).

One of the main features of the resistivity images is the occurrence of a high resistivity zone (>1000 Ωm) in both the N-S and WSW-ENE sections (see zones C and C1 in figures 5 and 6, respectively, as well as figure 8). This anomaly is delimited by the faults bordering the resurgent block. Considering the high heat flow and the elevated geothermal gradient of the area (Carlino *et al*., 2014), the relatively high resistivity anomaly (C and C1) can be explained in terms of permeability. High resistivity can be associated with a lower flow of hot hydrothermal fluids. This process, typical of many volcanic areas (Marsh, 1984), is related to the occurrence of crystalline rocks such as intrusive bodies with very low permeability (k) which ranges from 10^{-17} to 10^{-21} m^2 for granite, for example (Brace, 1980). Such low permeabilities would inhibit the passage of fluids because the minimum permeability for volatiles to transfer into the shallow crust is 10^{-20} to 10^{-18} m^2, while for fluid transfer the figure is ≥ 10^{-16} m^2 (Ingebritsen *et al*., 2010). Furthermore, geochemical and isotopic investigations (Tedesco, 1996) have highlighted the presence of magmatic fluids, which probably escape laterally from below to the magma body because they encounter a permeability barrier in a hugher more crystalline part. The presence of a shallow magmatic body (≈2 km in depth) beneath the Mount Epomeo resurgent structure, has already been inferred by other authors from interpretation of magnetic and gravity data (Nunziata and Rapolla, 1987; Paoletti *et al*, 2013 and references therein). For instance, the contemporary presence of a magnetic minimum and a gravimetric maximum (slightly decentred to the SW with respect to the centre of the island), might be explained by the existence of an intrusion or several intrusions and/or by partially melted zones to create pockets of crystal mush. This hypothesis is supported by the high temperature gradient measured in the central-western sector of the island (Penta and Conforto, 1951; Penta, 1954; Ippolito and Rapolla, 1982; Panichi *et al*., 1992; Paoletti *et al*., 2009). Furthermore, an undated intrusive rock was found at the bottom of the 1050 m deep drilling, located west of Mount Epomeo (well 2 in Figure 1) (Penta and Conforto, 1951; AGIP, 1987). Our findings seem to confirm the presence of such a shallow magmatic body with a bulge penetrating up to about 1 km below the surface. Furthermore, taking into account the geothermal gradient of the island (about 200°C km^{-1}) (see Carlino *et al*., 2012, 2014 for details) the solidus temperature (onset of melting) may be encountered at a depth >3 km.

As a whole, we are confident that this magmatic body represents an intrusion and cannot be related to other high resistivity structures, such as an uplifted basement or unfractured rocks filling the caldera. Further observations supporting our statement include: the high rate of resurgence of Mt. Epomeo, which indicates a magmatic process (injection) as driving mechanism (Tibaldi and Vezzoli, 2004; Sbrana *et al*., 2009) as driving mechanism; the observed pattern of deformation that can be associated with a shallow magmatic source with its top at about 2 km b.s.l. (Carlino, 2012); the observation that new trachybasaltic magma arrived in the shallow magmatic system before the volcanic activity 28-18 ka (Civetta *et al*., 1991); the melt inclusion data that reveal that the eruptive products of 73-59 ka came from a magmatic storage region located at a depth of about 2 km (Sbrana *et al*., 2009) and, finally, the very high geothermal gradient and high temperature hydrothermal system, associated with the presence of a shallow magmatic body (Sbrana *et al*., 2009; Carlino *et al*., 2012, 2014).

The resistivity anomaly (figure 8) perhaps thus represents the apex of a laccolith (or alternatively a series of cone sheets) (Westerman *et al*., 2004) intruded into the shallow crust of the island (Rittman, 1930; Sbrana *et al*., 2009; Paoletti *et al*., 2013; Carlino *et al*., 2006; Carlino, 2012), over the least 33 ka (Carlino, 2012 and references therein). Considering both the N-S and WSW-ENE profiles, the intrusion seems to have a branch that is elongated NS in the western sector of Mt. Epomeo.

Finally, we can compare the WSW-ENE profile with the geology of the island (*Carta Geologica dell'isola d'Ischia*, CARG project), which in this sector is mainly constrained by the stratigraphy revealed from the drilling (figure 10). As we seen in figure 10, around station I20 the resistivity anomaly (>2000 Ωm) corresponds to the Punta Imperatore lavas and to the eruptive center of Campotese (see also figure 1). These lavas, dated to about 177 ka (Gillot *et al*., 1982), are dissected by faults that possibly do not involve the more recent, overlying, deposits and that are associated with collapse of the caldera rim. The contrast in resistivity highlights the difference between the lower consolidated deposit of the inner caldera and the structural domes at the caldera rim. ENE to station I18 a very low resistivity area coincides with the most important fumarole field of the island (Bocca di Serra, Donna Rachele fumaroles). The fumarole field covers about 0.80 km^2 (80 hectares), with emissions totaling ≈ 9 td^{-1} (volume) of CO_2 that rise along a system of vertical faults (Chiodini *et al*., 2004). This system is perhaps partly fed by a relatively deep hydrothermal aquifer (about 600 m deep) (Chiodini *et al*., 2004), whose fluids take advantage of thethe structural discontinuity (faults and fractures system) located at the boundary of the uplifted block. We also note a coincidence between the variation in lithology encountered in the stratigraphy of the drillings (drillings 2 and 4, see figure 1 for location) (AGIP, 1987) and the variation in resistivity encountered in our cross-sections (figure 11a, b). Finally, in order to assess the influence of the intrusion on the tilting of the Mt. Epomeo block (Acocella and Funiciello, 1999) we need to improve our measurements to get a wider 3D imaging, because the resistivity anomalies seem to have a complex shape that cannot be well constrained by 2D inversion.

Discussion

Of the varying interpretations of the caldera resurgence process, the most common is that of magmatic intrusion which can evolve in a range of ways, from sills, to dikes or laccoliths(Paige, 1913; Henry *et al*., 1997; Acocella *et al*., 2001 and references therein). This process is generally associated with the formation of well-developed geothermal systems (Hulen et al., 1987).One implication of this study involves the mechanism producing resurgence of calderas. As in the case of Ischia, the relatively high rate of uplift, which provides a strain rate of at least one order of magnitude larger than tectonic processes (Carlino, 2012), excludes a regional tectonic contribution. The long-term rate of uplift makes it possible also to exclude any non-purely magmatic contribution to the resurgence, such as the oversaturation of volatile species in a shallow and crystallising magma body (Tait *et al*., 1989) or a fluid contribution (Hurwitz *et al.*, 2007). These processes are typically associated to relative small-scale (metres) and short-term (months to years) disturbances and, as in the case of the contribution of fluids, a partial recovery of the deformation occurring will take place (see, for instance, the example of Campi Flegrei caldera; Troiano *et al*., 2011 and references therein). The long-term resurgence of Ischia (from at least 33 ka to 5 ka) was punctuated by phases of quiescence (de Vita *et al*., 2010), which possibly corresponded to periods of volcanic activity (Carlino *et al*., 2006). However a large proportion of the magma arriving in the shallow system (Civetta *et al*., 1991) has not been erupted, and merely contributes to the uplift of Mt. Epomeo (Carlino *et al*. 2012), forming a very shallow intrusion whose occurrence seems to be confirmed by resistivity data. This behaviour is different when compared to that of the nearby Campi Flegrei caldera, (where some caldera sectors were uplifted by less than 100 m, while larger eruptions occurred). It is instead similar to the Grizzly Peak caldera (Colorado) (Fridrich et al., 1991) and Pantelleria (Southern Italy) (Orsi et al., 1991). In these cases, the rheology of the shallow magma sources and the response of the surrounding rock walls to the stress induced by the pressure of the magma possibly control the different evolutions of caldera resurgence. For instance, the temperature of the intruded magma and of the surrounding rock, together with the injection rate, strongly affect the behaviour of the system (Jellinek and DePaolo, 2003). Large geothermal gradients and low magma injection rates enhance creep processes instead of catastrophic failure, increasing the accretion of magma at depth and inhibiting eruptions (Jellinek and DePaolo, 2003). Overall, when the magma is the primary source of the resurgence of calderas, it is crucial to estimate its volume, thermal state and thermal history (Cooper and Kent, 2014), while the rheology of the magma itself and of the surrounding rock is critical in the evolution of the resurgence (Carlino and Somma, 2010). For the island of Ischia, if we assume a roughly radial symmetry of the resistivity anomaly associated with the magma intrusion (about 2 km in radius and 2 km in vertical extension), at least for the crust down to 3 km, that we obtain a magma volume of about 6 km^3. If this has been gathering since 33ka (Tibaldi and Vezzoli, 1998), then the accumulation rate is about $1.8 \cdot 10^{-4}$ km^3 a^{-1}.This possibly represents a lower limit of the volume of magma (and the magma rate) intruded into the shallow crust, which, in its present state (having been gathering over 33ka), is not likely to prove eruptible due to its thermal condition. That is the magma will be highly degassed and the maximum temperature is possibly ≤ 600°C (Carlino et al., 2014).

Conclusions

Our magnetotelluric survey carried out in the southern and western sector of the island of Ischia, detected several electrical resistivity anomalies, down to a depth of 3 km. The interpretation of the resistivity cross-sections and comparison with other geological, geophysical and geochemical data allow the following conclusions and inferences:

- a large thermal anomaly has been found in the southern and western sector of the island and is associated with a zone of heat advection and circulation of hydrothermal fluids (figures 5 and 6). The presence of two major hot aquifers, previously hypothesized by geochemical studies (Chiodini *et al*., 2004, Di Napoli *et al*., 2011), has also been located in the southwestern sector of the caldera. The aquifers reside at different depths, with the depths being controlled bytectonic movements, which have caused deformation of the resurgent block of Mt. Epomeo over at least the last 33 ka (Vezzoli, 1988). The top of the deeper aquifers feed the main south-western fumarole fields, and are located at a depth of about 1000 m to 1500 m, respectively;
- a large resistivity anomaly is located below the resurgent structure of Mt. Epomeo. It is interpreted as the apical part of a crystalline (and very low permeability) magmatic body intruded below the central part of the island (and slightly dislocated towards the south-west) and whose apex reaches a depth of about 1 km b.s.l. This body is bounded by an abrupt resistivity drop corresponding to the faults around to the resurgent block of Mt. Epomeo;
- we propose that this high resistivity body is associated with the laccolith of Ischia (Rittman, 1930; Sbrana *et al*., 2009; Carlino, 2012), which produced the bending, fracturing and faulting of the overlying crust, and which witnessedmagma intrusion during the most recent stage of the resurgence (5 ka) (Civetta *et al*., 1991; Vezzoli *et al*., 2009). As result, the uplifted block has been broken up into minor blocks, with the underlying laccolith possibly developing as a complex structure. This laccolith is the engine of the robust geothermal system of the island, and -to be consistent with a high resistivity - is likely dominated by a highly crystalline mush;
- the existence of such a shallow magma body is critical in terms of volcanic hazard assessment. The volcanism of Ischia seems, in fact, to be strictly correlated to the resurgence process that, in turn, is reliant on the dynamics of the laccolith (Carlino, 2012). A renewal of resurgence will be related to reactivation of the laccolith by arrival of new magma (Civetta *et al*., 1991).This may possibly produce a large disturbance of the geothermal system at a depth of between 1 km and 2 km. A reactivation of such a shallow magmatic system may imply imminent eruption and would pose high volcanic hazard (e.g. Cooper & Kent, 2014); certainly it would cause hydrothermal emissions to evolve towards magmatic (Vaselli et al., 2010).

Figures captions

Figure 1. Structural and geological map of Ischia Island (after Di Napoli *et al*., 2011). The MT measurement stations along the N-S profile are given as blue points; the MT measurement stations along the WSW-ENE profile are green points; the blue-green points are stations belonging to both the profiles; Drilling sites are given as red points numbered 1 to 5. The shaded grey circular area indicates the resurgence zone and black lines are mapped faults (Di Napoli et al. 2011). The dotted red lines indicate the resistivity section profiles.

Figure 2. Three examples of apparent resistivity and phase diagrams pertaining to the Ischia MT survey work.

Figure 3. (a) S-N Magnetotelluric profiles of apparent resistivity (above) and phase (below) pseudosections relative to the TM mode. (b) S-N Magnetotelluric profiles of apparent resistivity (above) and phase (below) pseudosections relative to the TE mode. (c) WSW-ENE magnetotelluric profiles of apparent resistivity (above) and phase (below) pseudosections relative to the TM mode. (d) WSW-ENE Magnetotelluric profiles of apparent resistivity (above) and phase (below) pseudosections relative to the TE mode (see text for details).

Figure 4. Results of the data dimensional analysis carried on the MT dataset using the phase tensor approach. The data have been divided up into four contiguous frequency bands, respectively centered on 0.9 9, 90 and 900 Hz. The phase- tensor ellipse orientation (in degrees) and the Caldwell-Bibby-Brown Skew angles are given, for each MT survey, in (panel a) and (panel b), respectively.

Figure 5. S-N resistivity profile obtained from the inversion of the MT survey (panel b). Dotted lines are the faults associated with the caldera boundary and to the dislocation of the resurgent block (see text for details). It is also reported (panel a) the topographic profile along the section.

Figure 6. WSW-ENE resistivity profile obtained from the inversion of the MT survey (panel b). The resistivity anomalies (marked as E, E1 and E2) is coincident with a thermal plume producing high geothermal gradients and very high temperatures (~100°C) at the surface (Carlino et al., 2014). It is also reported (panel a) the topographic profile along the section.

Figure 7. Sensitivity cross-sections relative to the resistivity models (S-N profile, above and WSW-ENE profile, below).

Figure 8. Topography in shaded relief of Ischia draped over the DEM (INGV web-GIS source), perspective views from W (a), NE (b), SW (c), S (d). Beneath each are the resistivity data for the two profiles so as to set in context the variations we record with depth, as well as distance from Mt. Epomeo."

Figure 9. Magnification of the central part of the WSW-ENE profile compared with the geotherms (after Carlino et al., 2014)

Figure 10. Comparison of the shallower part of WSE-ENE resistivity profile with a geological section of the island (from *Carta Geologica dell'Isola d'Ischia*, CARG project). *Legend: PZE = Pizzone Tuffs (~61 ka); TFS = Frassitelli Tuffs (~62 ka);VNU = dike and tabular intrusions; TME = Mount Epomeo Green Tuff (~55 ka); PIM-FGN = Punta Imperatore ancient lavas (~117 ka); ELF = Elephant pyroclastic deposits; TCT = Citara Tuffs (~45 Ka);SUN = debris and mud flow deposits; PPI = Punta Imperatore pyroclastic deposits (~ 18 ka); PUS = Punta Soccorso debris avalanche;* a_{ta} *= alluvial deposits. (from CARG project)*

Figure 11 (a, b). Magnification of the sections given in figures 5 and 6 with the position od drill sites 2 and 4 (see figure 1 for location) from which stratigraphic data are taken. Legend: (drill n. 4) VB = Volcanic Breccia; GT = Green Tuff; GTL = Green Tuff interlayered with trachytic lava. (drill n. 2) RT = Reworked Tuffs and Alluvium; TYT = Trachytic Yellow Tuffs; PLD = Pyroclastic and Lava deposits; GrT = Green Tuff; TL = Trachytic lava

Acknowledgements: This work was carried out in the framework of the INGV-DPC Research Agreement 2012–2021 "All. A". We are grateful to the Associate Editor, V. Acocella, the Executive Editor, A. Harris, and to the Referees, J. Stix and A. Revil, for their helpful comments that have greatly improved the quality of the work.

References

Abdul Azeez K, Harinarayana, T (2007) Magnetotelluric evidence of potential geothermal resource in Puga, Ladakh, NW Himalaya. Curr. Sci., 93, 323–329.

Acocella V, & Funiciello R (1999) The interaction between regional and local tectonics during resurgent doming: the case of the island of Ischia, Italy. Journal of Volcanology and Geothermal Research, 88(1), 109-123.

Acocella V, Cifelli F, & Funiciello R (2001) The control of overburden thickness on resurgent domes: insights from analogue models. Journal of Volcanology and Geothermal Research, 111(1), 137-153.

AGIP (1987) Geologia e geofisica del sistema geotermico dei Campi Flegrei, Technical report, Settore Esplor e Ric Geoterm-Metodol per l'Esplor Geotermica, San Donato Milanese Italy, pp 1–23

Arango C, Marcuello A, Ledo J, Queralt P (2009) 3D magnetotelluric characterization of the geothermal anomaly in the Llucmajor aquifer system (Majorca, Spain). J. Appl. Geophys., 68 (4), 479–488.

Bai, D., Meju, M. A., & Liao, Z. (2001). Magnetotelluric images of deep crustal structure of the Rehai geothermal field near Tengchong, southern China. Geophysical Journal International, 147(3), 677-687.

Barra, D., Cinque, A., Italiano, A., & Scorziello, R. (1992). Il Pleistocene superiore marino di Ischia: paleoecologia e rapporti con l'evoluzione tettonica recente. Studi geologici Camerti, 1(special issue), 231-243 (*in italian*)

Brace W F (1980, October) Permeability of crystalline and argillaceous rocks. In International Journal of Rock Mechanics and Mining Sciences & Geomechanics Abstracts (Vol. 17, No. 5, pp. 241-251). Pergamon.

Berdichevsky, M. N., & Dmitriev, V. I. (2010). Models and methods of magnetotellurics. Springer Science & Business Media.

Booker, J. R. (2014). The magnetotelluric phase tensor: a critical review. Surveys in Geophysics, 35(1), 7-40.

Brasse, H., & Soyer, W. (2001). A magnetotelluric study in the Southern Chilean Andes. Geophysical Research Letters, 28(19), 3757-3760.

Caldwell T, Grant H, Bibby M, Brown C (2004) The magnetotelluric phase tensor. Geophys. J. Int. 158, 457–469.

Carlino S, Cubellis E, Luongo G, Obrizzo F (2006). On the mechanics of caldera resurgence of Ischia Island (southern Italy). Geological Society, London, Special Publications, 269(1), 181-193.

Carlino S, and Somma R (2010) Eruptive versus non-eruptive behaviour of large calderas: the example of Campi Flegrei caldera (southern Italy), Bulletin of Volcanology, 72(7), 871–886

Carlino S (2012) The process of resurgence for Ischia Island (southern Italy) since 55 ka: the laccolith model and implications for eruption forecasting. Bulletin of Volcanology, 74(5), 947-961.

Carlino S, Somma R, Troise C, De Natale G (2012) The geothermal exploration of Campanian volcanoes: Historical review and future development. Renewable and Sustainable Energy Reviews, 16(1), 1004-1030.

Carlino S, Somma R, Troiano A, Di Giuseppe M G, Troise C, De Natale G (2014). The geothermal system of Ischia Island (southern Italy): critical review and sustainability analysis of geothermal resource for electricity generation. Renewable Energy, 62, 177-196.

Carlino S, Somma R, Troiano A, Di Giuseppe M G, Troise C, & De Natale G (2015) Geothermal Investigations of Active Volcanoes: The Example of Ischia Island and Campi Flegrei Caldera (Southern Italy). In Engineering Geology for Society and Territory-Volume 1 (pp. 369-372). Springer, Cham.

Carrara E, Pinna E, & Rapolla A (1983) Indagini geofisiche nelle aree vulcaniche italiane di interesse geotermico. Atti Accademia Pontaniana, Nuova Serie, XXXI, 299–314.

CARG project (2011) Carta Geologica dell'Isola d'Ischia , Regione Campania.

Celico P, Stanzione D, Esposito L, Formica F, Piscopo V, De Rosa B M (1999) La complessità idrogeologica di un'area vulcanica attiva; l'Isola d'Ischia (Napoli, Campania). Bollettino della Società Geologica Italiana, 118(3), 485-504.

Chang W L, Smith R B, Farrell J, & Puskas C M (2010) An extraordinary episode of Yellowstone caldera uplift, 2004–2010, from GPS and InSAR observations. Geophysical Research Letters, 37(23).

Chiodini G, Avino R, Brombach T, Caliro S, Cardellini C, de Vita S,.... & Ventura G (2004) Fumarolic and diffuse soil degassing west of Mount Epomeo, Ischia, Italy. Journal of Volcanology and Geothermal Research, 133(1), 291-309.

Civetta L, Gallo G, Orsi G (1991) Sr-and Nd-isotope and trace-element constraints on the chemical evolution of the magmatic system of Ischia (Italy) in the last 55 ka. Journal of Volcanology and Geothermal Research, 46(3), 213-230.

Cooper K M, & Kent A J (2014). Rapid remobilization of magmatic crystals kept in cold storage. Nature, 506(7489), 480.

de Vita S, Sansivero F, Orsi G, Marotta E, Piochi M (2010) Volcanological and structural evolution of the Ischia resurgent caldera (Italy) over the past 10 ky. Geological Society of America Special Papers, 464, 193-239.

De Martino, Tammaro U, ObrizzoF, Sepe V, Brandi G, D'Alessandro, DolceM, Pingue F (2011) La Rete GPS dell'isola di Ischia: deformazioni del suolo in un'area vulcanica attiva (1998-2010). Quaderni di Geofisica, n.92.

Di Giuseppe M G, Troiano A, Fedele A, Caputo T, Patella D, Troise C, De Natale G (2015) Electrical resistivity tomography imaging of the near-surface structure of the Solfatara Crater, Campi Flegrei (Naples, Italy). Bulletin of Volcanology, 77(4), 27.

Di Giuseppe, M. G., Troiano, A., & Patella, D. (2017a). Separation of plain wave and near field contributions in Magnetotelluric time series: A useful criterion emerged during the Campi Flegrei (Italy) prospecting. Journal of Applied Geophysics. doi: 10.1016/j.jappgeo.2017.03.019.

Di Giuseppe M G, Troiano A, Di Vito M A, Somma R, & Matano F (2017b) Definition of small-scale volcanic structures by Electrical Resistivity Tomography: the Trentaremi cone, an example from the Campi Flegrei Caldera (Italy). Annals of Geophysics, 60(5), 0552.

Di Giuseppe M G, Troiano A, Patella D, Piochi M, & Carlino S (2017c). A geophysical k-means cluster analysis of the Solfatara-Pisciarelli volcano-geothermal system, Campi Flegrei (Naples, Italy). Journal of Applied Geophysics.

Di Napoli R, Aiuppa A, Bellomo S, Brusca L, D'Alessandro W, Gagliano Candela E, Longo M, Pecoraino G, Valenza M (2009) A model for Ischia hydrothermal system: evidences from the chemistry of thermal groundwaters. Journal of Volcanology and Geothermal Research, 186(3), 133-159.

Di Napoli R, Martorana R, Orsi G, Aiuppa A, Camarda M, De Gregorio Gagliano Candela E, Luzio D, Messina N, Pecoraino G, Bitetto M, de Vita S, Valenza M (2011) The structure of a hydrothermal system from an integrated geochemical, geophysical, and geological approach: The Ischia Island case study. Geochemistry, Geophysics, Geosystems, 12(7).

Egbert G D, Booker J R (1986) Robust estimation of geomagnetic transfer functions. Geophysical Journal International, 87(1), 173-194.

Egbert, G. D., & Livelybrooks, D. W. (1996). Single station magnetotelluric impedance estimation: Coherence weighting and the regression M-estimate. Geophysics, 61(4), 964-970.

Fridrich CJ, Smith RP, DeWitt E, McKee EH (1991) Structural, eruptive, and intrusive evolution of the Grizzly Peak caldera, Sawatch Range, Colorado. Geol Soc Am Bull 103 : 1160–1177.

Fusi N, Tibaldi A, Vezzoli L (1990) Vulcanismo, risorgenza calderica e relazioni con la tettonica regionale nell’isola d’Ischia. Memorie della Società Geologica Italiana, 45, 971-980.

Gillot P Y, Chiesa, S, Pasquare G, & Vezzoli L (1982). < 33,000-yr K–Ar dating of the volcano–tectonic horst of the Isle of Ischia, Gulf of Naples. Nature, 299(5880), 242-245.

Heise W, Caldwell T G, Bibby H M, Bannister S C (2008) Three-dimensional modelling of magnetotelluric data from the Rotokawa geothermal field, Taupo Volcanic Zone, New Zealand. Geophys. J. Int., 173 (2), 740–750.

Henry, C D, Kunk, M J, Muehlberger, W R, Mcintosh, W C (1997) Igneous evolution of a complex laccolith–caldera, the Solitario, Trans- Pecos. Texas: implications for calderas and subjacent plutons. GSA Bulletin, 109, 1036–1054.

Hulen J B, Nielson D L, Goff F, Gardner J N, & Charles R W (1987) Molybdenum mineralization in an active geothermal system, Valles caldera, New Mexico. Geology, 15(8), 748-752.

Hurwitz S, Christiansen L B, & Hsieh P A (2007) Hydrothermal fluid flow and deformation in large calderas: Inferences from numerical simulations. Journal of Geophysical Research: Solid Earth, 112(B2).

Ingebritsen S E, Geiger S, Hurwitz S, Driesner T (2010). Numerical simulation of magmatic hydrothermal systems. Reviews of Geophysics, 48(1).

Ippolito F, Rapolla A, (1982) L'energia geotermica in Campania. Fonti Energetiche Alternative, Fondazione Politecnica per il Mezzogiorno. Franco Angeli Ed., Milan, pp. 57–106 (in Italian).

Jardani A, Revil A. Bolève A. & Dupont J P (2008), 3D inversion of self-potential data used to constrain the pattern of ground water flow in geothermal fields, Journal of Geophysical Research, 113, B09204, doi: 10.1029/2007JB005302.

Jellinek A M, & DePaolo D J (2003) A model for the origin of large silicic magma chambers: precursors of caldera-forming eruptions. Bulletin of Volcanology, 65(5), 363-381.

Jones, A G (1988) Static shift of magnetotelluric data and its removal in a sedimentary basin environment. Geophysics, 53(7), 967-978.

Kawakami Y, Hoshi H, & Yamaguchi Y (2007) Mechanism of caldera collapse and resurgence: observations from the northern part of the Kumano acidic rocks, Kii peninsula, southwest Japan. Journal of Volcanology and Geothermal Research, 167(1), 263-281.

Kelbert A, Meqbel N, Egbert G D, & Tandon K (2014) ModEM: a modular system for inversion of electromagnetic geophysical data. Computers & Geosciences, 66, 40-53.

Kennedy B, & Stix J (2007) Magmatic processes associated with caldera collapse at Ossipee ring dyke, New Hampshire. Geological Society of America Bulletin, 119(1-2), 3-17.

Kennedy B, Wilcock J, & Stix J (2012) Caldera resurgence during magma replenishment and rejuvenation at Valles and Lake City calderas. Bulletin of volcanology, 74(8), 1833-1847.

Kilburn C R (2003) Multiscale fracturing as a key to forecasting volcanic eruptions. Journal of Volcanology and Geothermal Research, 125(3), 271-289.

Ledo J, Queralt P, Martí A, & Jones A G (2002) Two-dimensional interpretation of three-dimensional magnetotelluric data: an example of limitations and resolution. Geophysical Journal International, 150(1), 127-139.

Marsh B D (1984) On the mechanics of caldera resurgence. Journal of Geophysical Research: Solid Earth, 89(B10), 8245-8251.

McNeice G W, Jones A G (2001) Multisite, multifrequency tensor decomposition of magnetotelluric data. Geophysics 66, 158–173.

Nunziata C, Rapolla A (1987) A gravity and magnetic study of the volcanic island of Ischia, Naples (Italy). Journal of volcanology and geothermal research, 31(3-4), 333-344.

G. Orsi, G. Gallo, A. Zanchi (1991) Simple-shearing block resurgence in caldera depressions. A model from Pantelleria and Ischia J. Volcanol. Geotherm. Res., 47, pp. 1-11

Paige, S (1913) The bearing of progressive increase of viscosity during intrusion on the form of laccoliths. The Journal of Geology, 21(6), 541-549.

Panichi C, Bolognesi L, Ghiara M R, Noto P, Stanzione D(1992) Geothermal assessment of the island of Ischia (southern Italy) from isotopic and chemical composition of the delivered fluids. J. Volcanol. Geotherm. Res. 49, 329–348.

Paoletti V, Di Maio R, Cella F, Florio G, Motschka K, Roberti N, ... & Rapolla A (2009) The Ischia volcanic island (Southern Italy): Inferences from potential field data interpretation. *Journal of Volcanology and Geothermal Research*, *179*(1), 69-86.

Paoletti V, D'Antonio M, & Rapolla A (2013) The structural setting of the Ischia Island (Phlegrean Volcanic District, Southern Italy): inferences from geophysics and geochemistry. Journal of Volcanology and Geothermal Research, 249, 155-173.

Pedersen L B, & Engels M (2005). Routine 2D inversion of magnetotelluric data using the determinant of the impedance tensor. Geophysics, 70(2), G33-G41.

Penta F (1954) Ricerche e studi sui fenomeni esalativi-idrotermali e il problema delle forze endogene. Ann. Geofis. 8, 1–94 (in Italian).

Penta F (1963) Sulle caratteristiche idrotermologiche dell'isola d'Ischia(Napoli). Rendiconti dell'Accademia dei Lincei, 34, 1-8 (in Italian).

Penta F, Conforto B (1951) Sulle trivellazioni in aree idrotermali per ricerche di vapore. L" ingegnere, Riv. Tecn. Mens. Ass. Naz. Ingg. Archt. It., Milano, 3, 12 (in Italian).

Pollard, D D, & Johnson, A M (1973). Mechanics of growth of some laccolithic intrusions in the Henry Mountains, Utah, II: bending and failure of overburden layers and sill formation. Tectonophysics, 18(3-4), 311-354.

Pous J, Heise W, Schnegg P A, Muñoz G, Martí J, & Soriano C (2002) Magnetotelluric study of the Las Canadas caldera (Tenerife, Canary Islands): structural and hydrogeological implications. Earth and Planetary Science Letters, 204(1), 249-263

Ranganayaki R P (1984) An interpretive analysis of magnetotelluric data. Geophysics 49, 1730–1748.

Rao C K, Jones A G, Moorkamp M (2007) The geometry of the Iapetus Suture Zone in central Ireland deduced from a magnetotelluric study. Phys. Earth Planet. Inter., 161, 134–141.

Revil A, Hermitte D. Spangenberg E, &. Cochémé J J (2002) Electrical properties of zeolitized volcaniclastic materials, Journal of Geophysical Research, 107(B8), 2168, 10.1029/2001JB000599

Revil A, Johnson T C, and Finizola A (2010) Three-dimensional resistivity tomography of Vulcan's forge, Vulcano Island, southern Italy, Geophys. Res. Lett., 37, L15308, doi:10.1029/2010GL043983, 2010

Revil A, Le Breton M, Niu Q, Wallin E, Haskins E, and Thomas D M (2017) Induced polarization of volcanic rocks. 1. Surface versus quadrature conductivity, Geophysical Journal International, 208, 826-844 doi: 10.1093/gji/ggw444.

Revil A, Le Breton M, Niu Q, Wallin E. Haskins E. and Thomas D M (2017) Induced polarization of volcanic rocks. 2. Influence of pore size and permeability, Geophysical Journal International, 208, 814-825 doi: 10.1093/gji/ggw382.

Rinaldi A P, Todesco M, Vandemeulebrouck J, Revil A, Bonafede M (2011) Electrical conductivity, ground displacement, gravity changes, and gas flow at Solfatara crater (Campi Flegrei caldera, Italy): Results from numerical modeling, Journal of Volcanology and Geothermal Research, 207 (3-4) 93-105,

Rittmann A (1930) Geologie der Insel Ischia, Z. Vulkanol. Ergbon, (6), pp 1-265

Rosenkjaer G K, Gasperikova E, Newman G A, Arnason K, & Lindsey N J (2015) Comparison of 3D MT inversions for geothermal exploration: Case studies for Krafla and Hengill geothermal systems in Iceland. Geothermics, 57, 258-274.

Saunders S J (2001) The shallow plumbing system of Rabaul caldera: a partially intruded ring fault?. Bulletin of volcanology, 63(6), 406-420.

Sbrana A, Fulignati P, Marianelli P, Boyce A J, Cecchetti A (2009) Exhumation of an active magmatic–hydrothermal system in a resurgent caldera environment: the example of Ischia (Italy). Journal of the Geological Society, 166(6), 1061-1073.

Schön J H (2015) Physical properties of rocks: Fundamentals and principles of petrophysics (Vol. 65). Elsevier.

Schwalenberg K, Rath V, Haak V (2002) Sensitivity studies applied to a two-dimensional resistivity model from the Central Andes. Geophys. J. Int., 150, 673–686.

Sepe V, Atzori S, Ventura G (2007) Subsidence due to crack closure and depressurization of hydrothermal systems: a case study from Mt Epomeo (Ischia Island, Italy). Terra Nova, doi: 10.1111/j.1365-3121.2006.00727.x

Simpson F, Bahr K (2005) Practical magnetotellurics. Cambridge University Press.

Siripunvaraporn, W., Egbert, G., Lenbury, Y., Uyeshima, M., 2005a. Three-dimensional magnetotelluric inversion: data-space method. Phys. Earth Planet. Inter. 150, 3–14.

Siripunvaraporn, W., Egbert, G., & Uyeshima, M. (2005b). Interpretation of two-dimensional magnetotelluric profile data with three-dimensional inversion: synthetic examples. Geophysical Journal International, 160(3), 804-814.

Smith R L, and Bailey R A (1969) Resurgent Cauldrons. U.S.G.S., Washington. The Geological Society of America, Memoir 116: 613-662.

Tait S, Jaupart C, & Vergniolle S (1989) Pressure, gas content and eruption periodicity of a shallow, crystallising magma chamber. Earth and Planetary Science Letters, *92*(1), 107-123.

Tedesco D (1996) Chemical and isotopic investigations of fumarolic gases from Ischia Island (southern Italy); evidences of magmatic and crustal contribution J. Volcanol. Geotherm. Res., 74, pp. 233-242

Tibaldi A, & Vezzoli L (1998) The space problem of caldera resurgence: an example from Ischia Island, Italy. Geologische Rundschau, 87(1), 53-66.

Tibaldi A, Vezzoli L (2004) A new type of volcano flank failure: the resurgent caldera sector collapse, Ischia, Italy. Geophysical Research Letters, 31(14).

Troiano A, Petrillo Z, Di Giuseppe M G, Balasco M, Diaferia I, Di Fiore B, Siniscalchi A, Patella D (2008) About the shallow resistivity structure of Vesuvius volcano. Ann. Geophys. 51, 179–187.

Troiano A, Di Giuseppe M G, Petrillo Z, Patella D (2009) Imaging 2D structures by the CSAMT method. Application to the Pantano di S. Gregorio Magno faulted basin (Southern Italy). J. Geophys. Eng. 6, 120–130.

Troiano A, Di Giuseppe M G, Petrillo Z, Troise C, & De Natale G (2011) Ground deformation at calderas driven by fluid injection: modelling unrest episodes at Campi Flegrei (Italy). Geophysical Journal International, 187(2), 833-847.

Troiano A, Di Giuseppe M G, Patella D, Troise C, De Natale G (2014) Electromagnetic outline of the solfatara–pisciarelli hydrothermal system, campi flegrei (southern italy). Journal of Volcanology and Geothermal Research, 277, 9-21.

Vaselli O, Tassi F, Duarte E, Fernández E, Poreda R, Huertas J (2010) Evolution of fluid geochemistry at the Turrialba volcano (Costa Rica) from 1998 to 2008. Bull Volcan 72(4), 397–410

Vezzoli L (1988) Island of Ischia. Quaderni de ‘La Ricerca Scientifica’. Consiglio Nazionale Ricerche Roma 114(10):7–126

Vezzoli L, Principe C, Malfatti J, Arrighi S, Tanguy J C, Le Goff M (2009) Modes and times of caldera resurgence: the< 10 ka evolution of Ischia Caldera, Italy, from high-precision archaeomagnetic dating. Journal of Volcanology and Geothermal Research, 186(3), 305-319

Vozoff K (1991) The magnetotelluric method. In: Nabighian, M.N. (Ed.), Electromagnetic Methods in Applied Geophysics. Application, vol. 2B. Society of Exploration Geophysicists, Tulsa, OK, pp. 641–711.

Weaver J T, Agarwal A K, Lilley F E M (2000) Characterization of the magnetotelluric tensor in terms of its invariants. Geophys. J. Int. 141, 321–336.

Westerman D S, Dini A, Innocenti F, & Rocchi S (2004) Rise and fall of a nested Christmas-tree laccolith complex, Elba Island, Italy. Geological Society, London, Special Publications, 234(1), 195-213.

Yang B, Egbert G D, Kelbert A, & Meqbel N M (2015) Three-dimensional electrical resistivity of the north-central USA from EarthScope long period magnetotelluric data. Earth and Planetary Science Letters, 422, 87-93.

Figure 1

Click here to download Figure Figure_1.tif

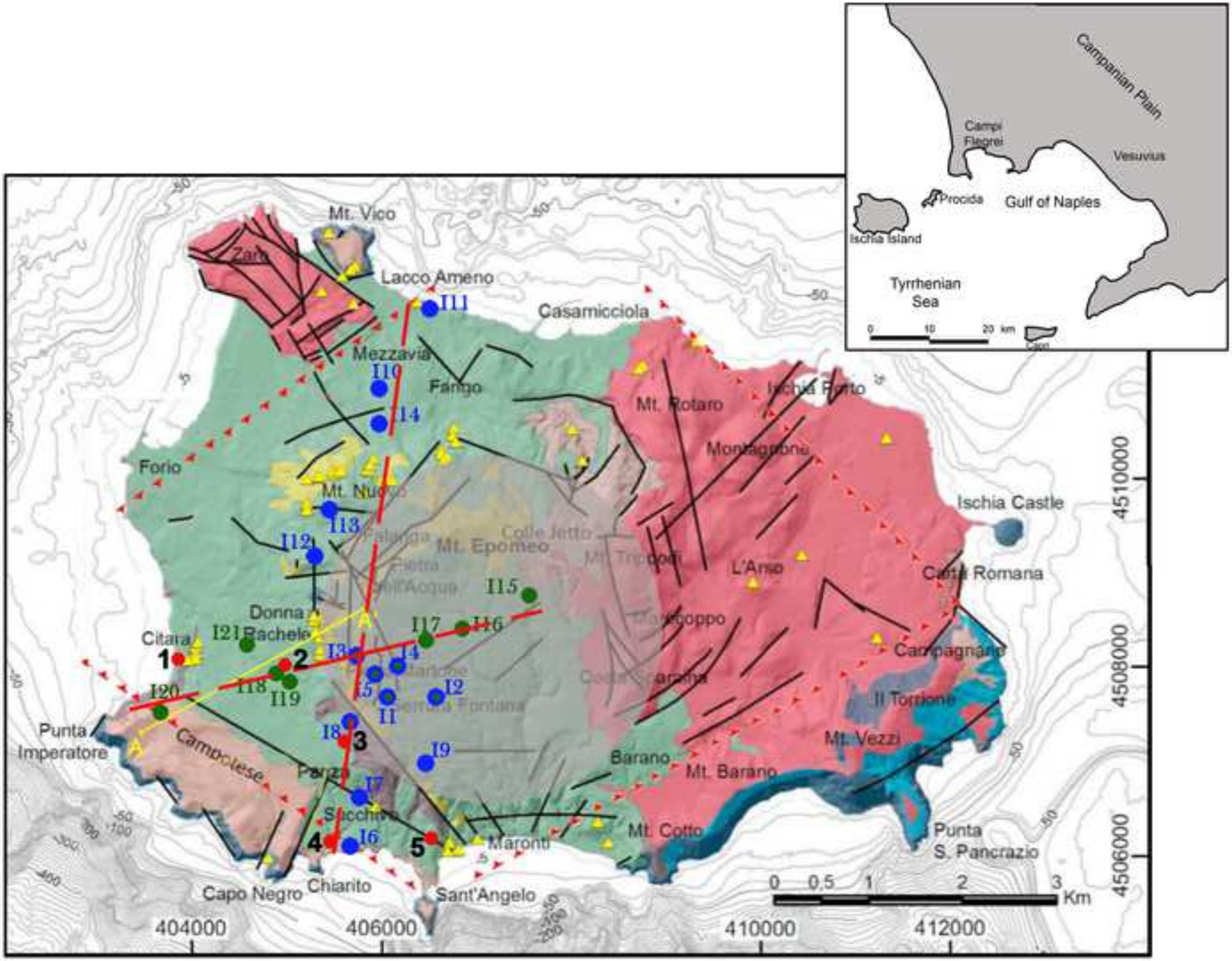

Figure 1 legend

Click here to download Figure Figure_1_legend.tif

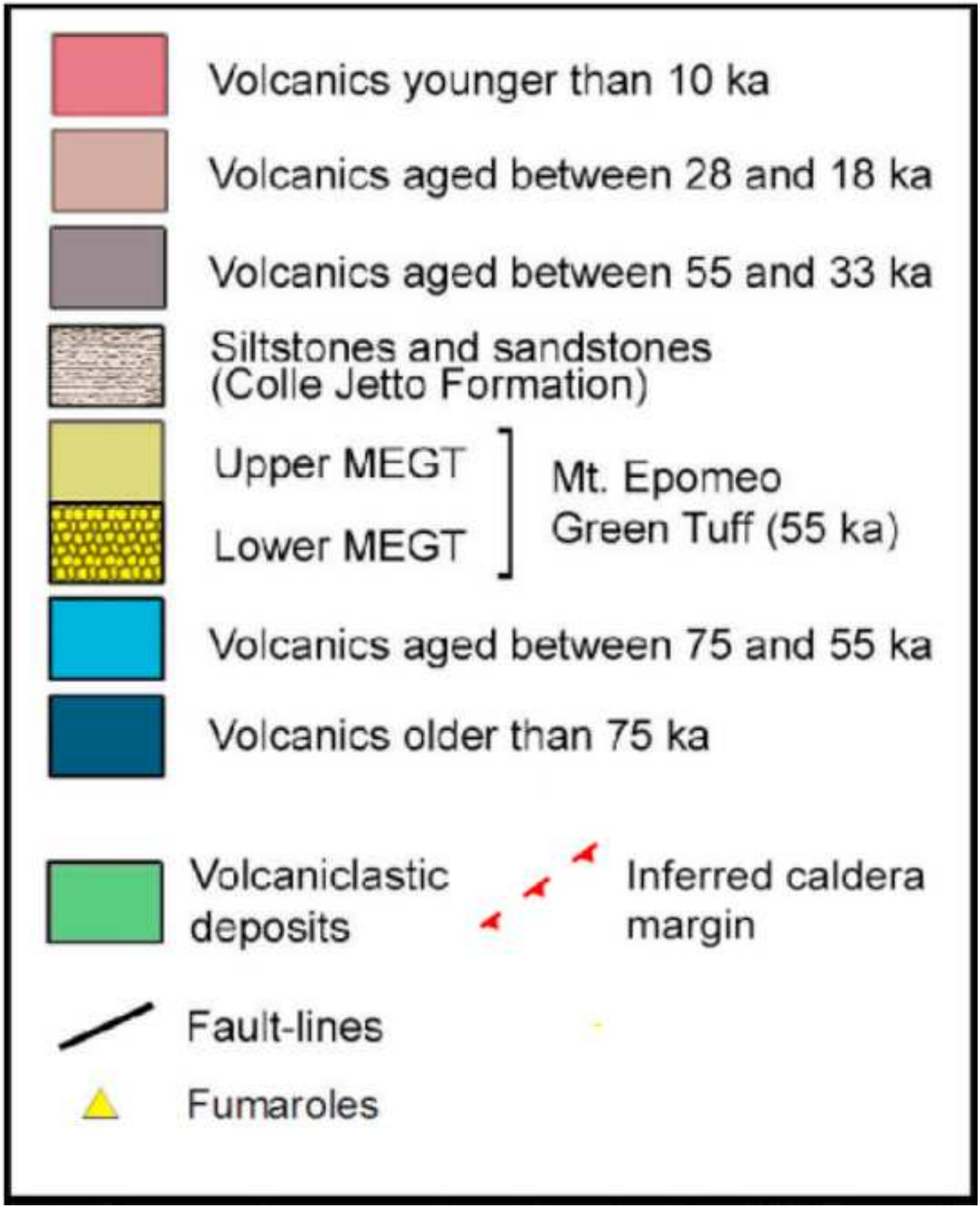

Figure 2

Click here to download Figure Figure_2.jpg

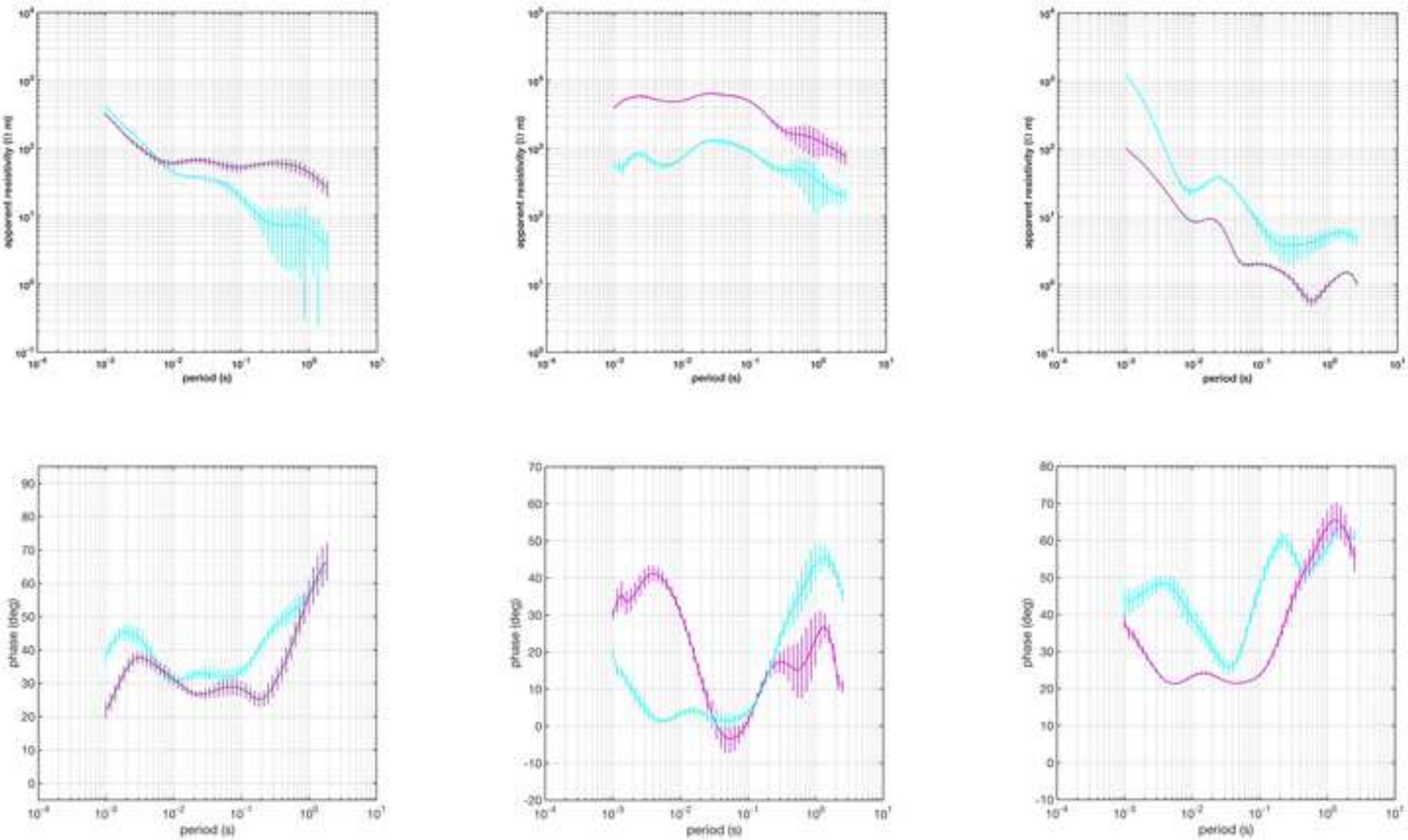

Figure 3 Click here to download Figure Figure_3.tif

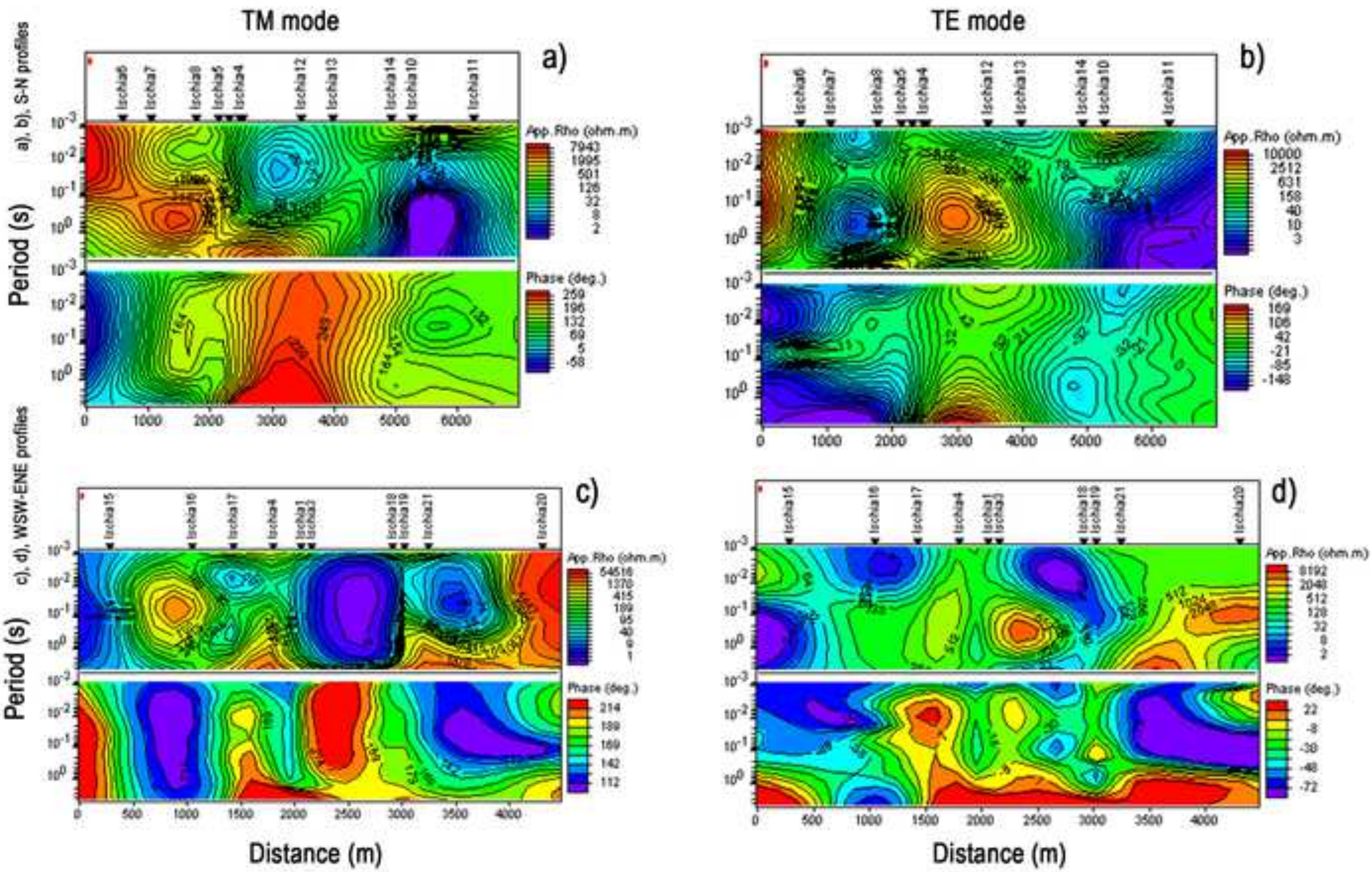

Figure 4

Click here to download Figure Figure_4.jpg

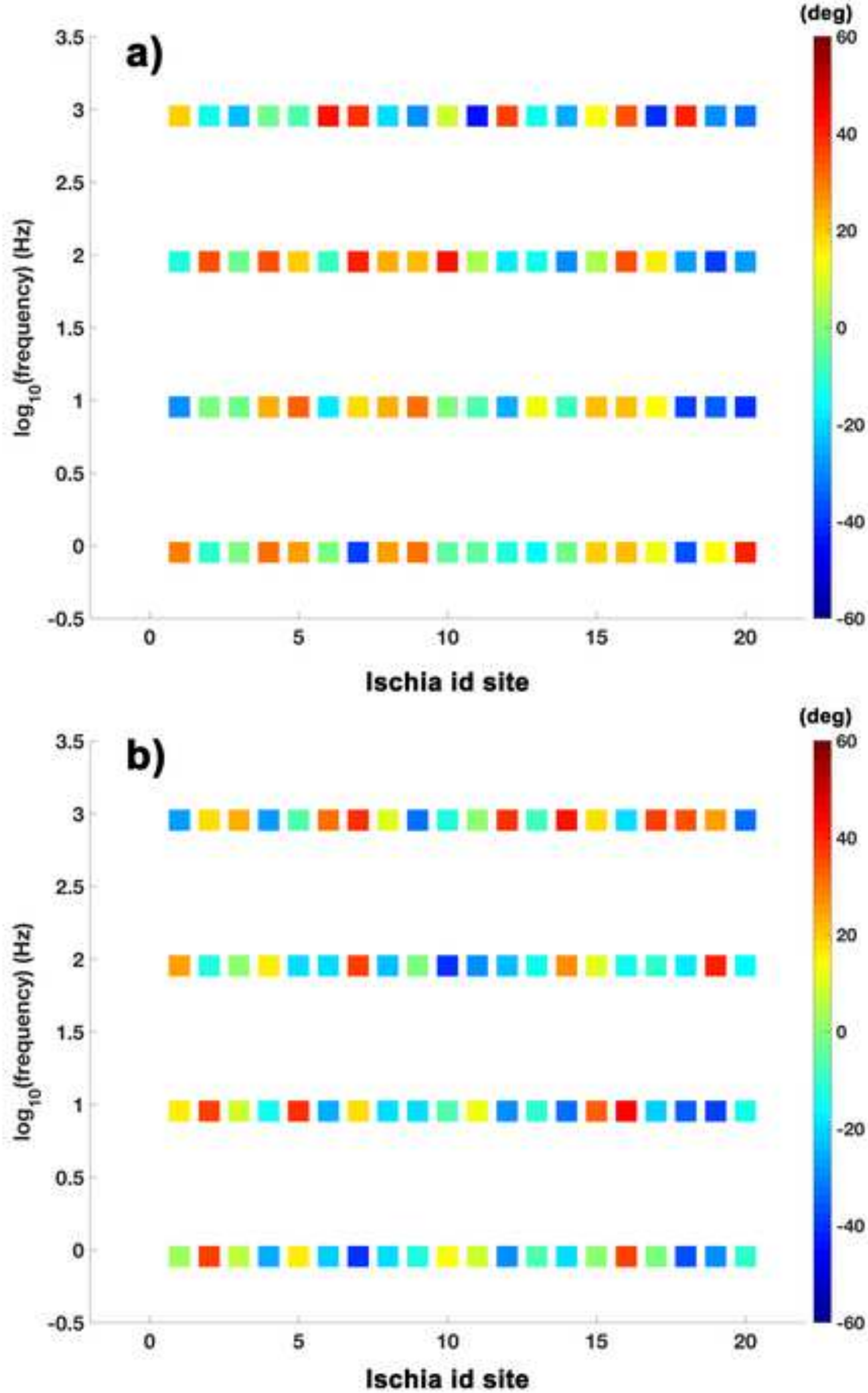

Figure 5

Click here to download Figure Figure_5.tif

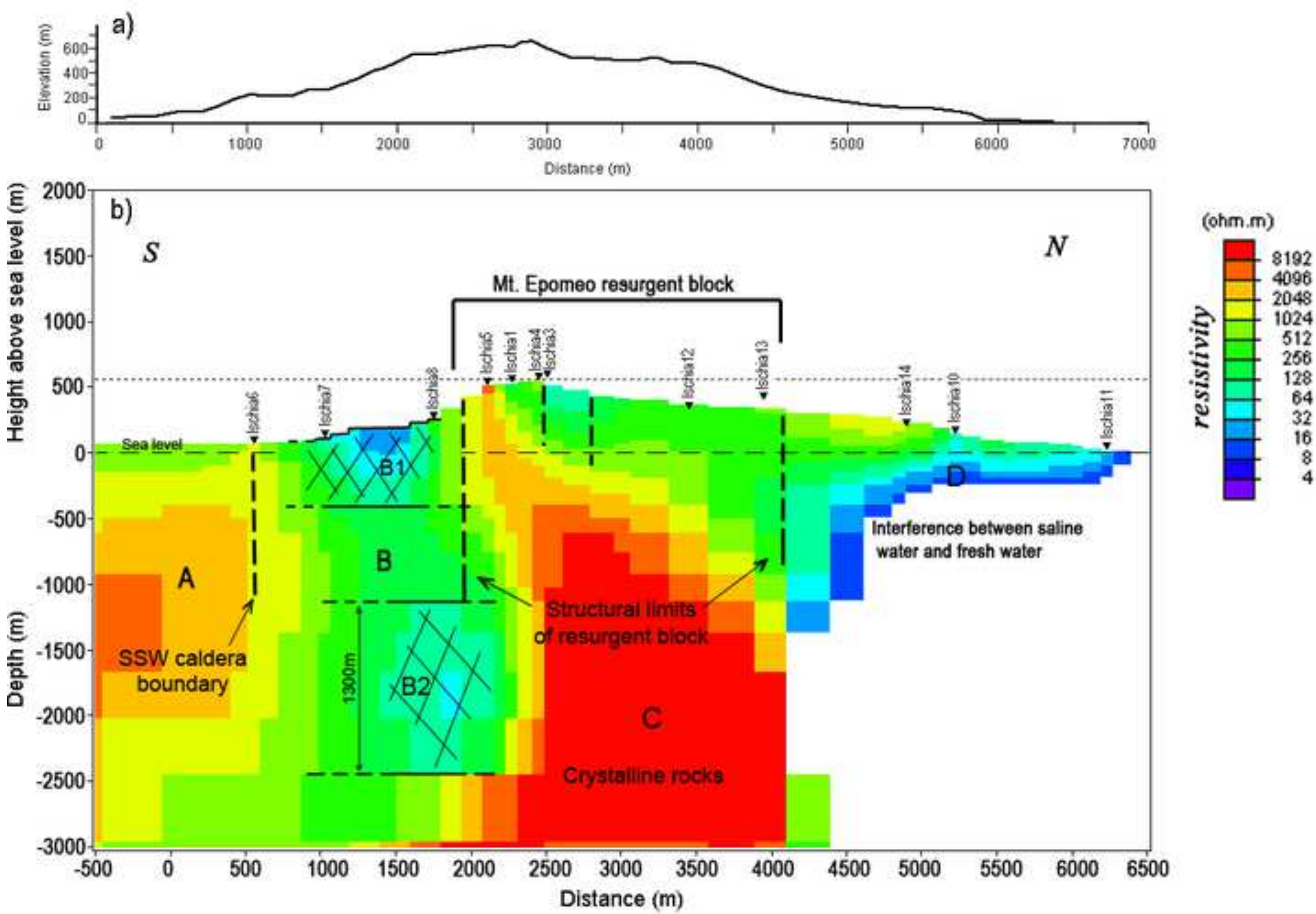

Figure 6

Click here to download Figure Figure_6.tif

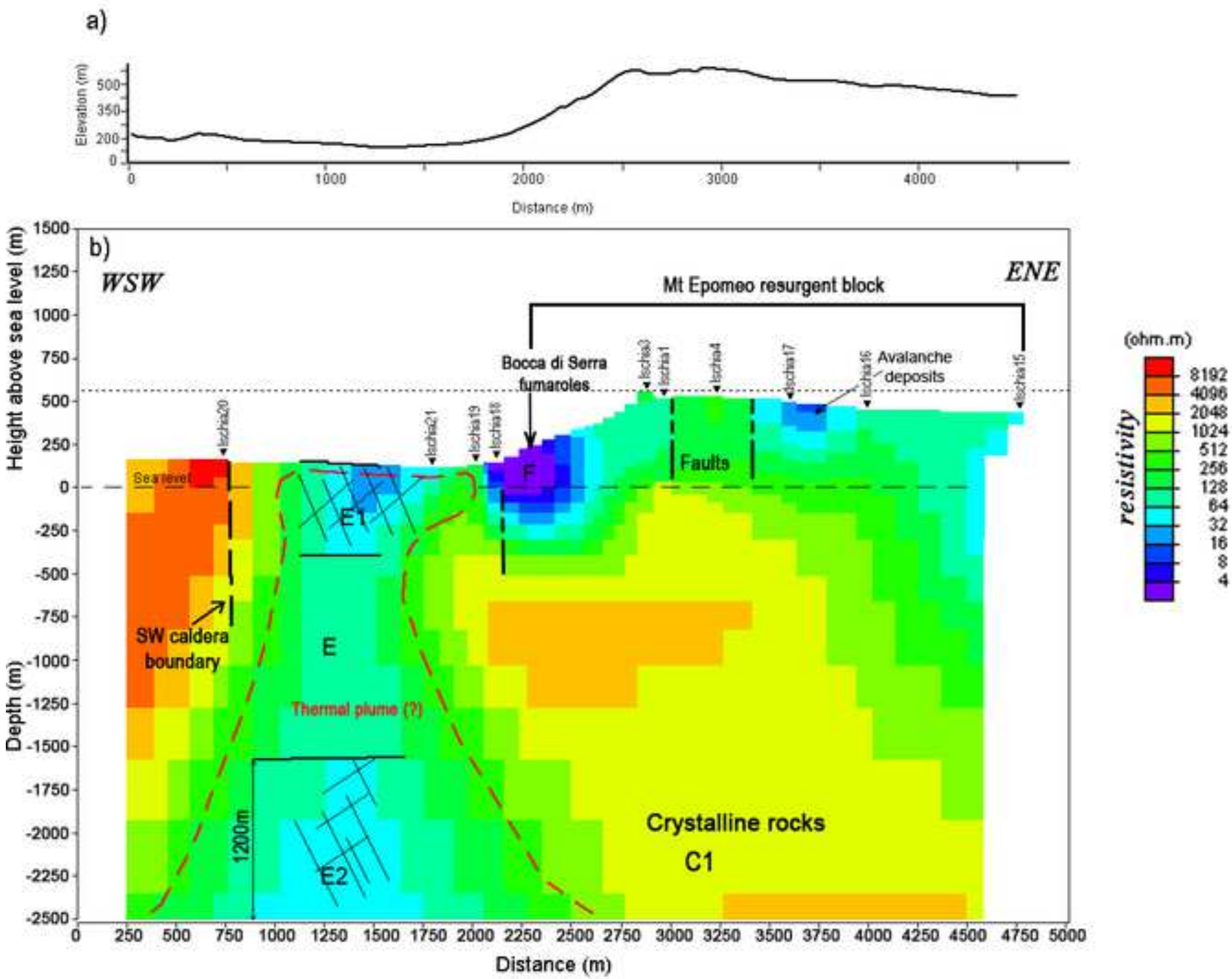

Figure 7

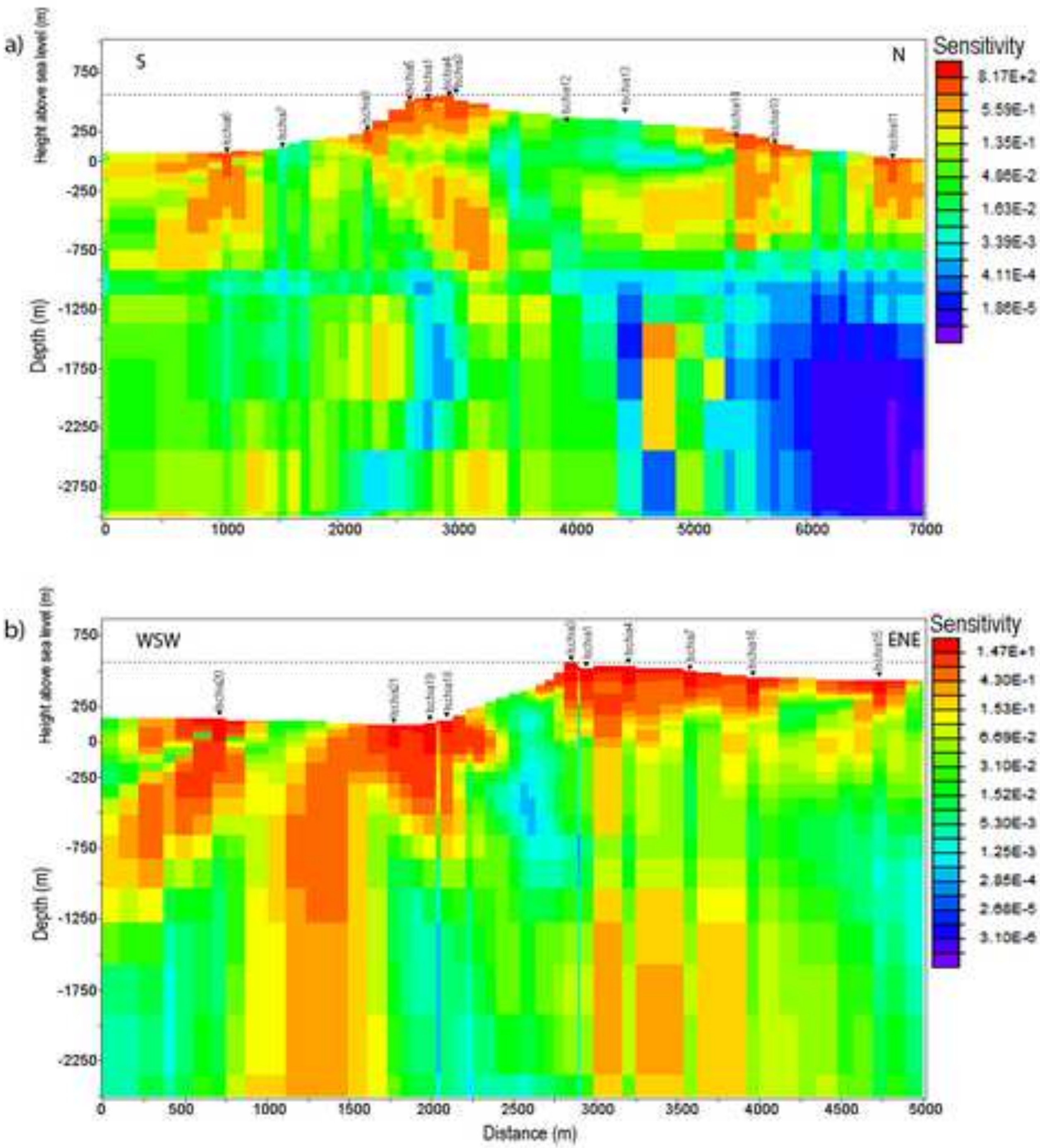
a)
S
N
Sensitivity
8.17E+2
5.59E-1
1.35E-1
4.85E-2
1.63E-2
3.39E-3
4.11E-4
1.86E-5
Height above sea level (m)
Depth (m)
750
250
0
-250
-750
-1250
-1750
-2250
-2750
0
1000
2000
3000
4000
5000
6000
7000
b)
WSW
ENE
Sensitivity
1.47E+1
4.30E-1
1.53E-1
6.69E-2
3.10E-2
1.52E-2
5.30E-3
1.25E-3
2.85E-4
2.68E-5
3.10E-6
Height above sea level (m)
Depth (m)
750
250
0
-250
-750
-1250
-1750
-2250
0
500
1000
1500
2000
2500
3000
3500
4000
4500
5000
Distance (m)

Figure 8

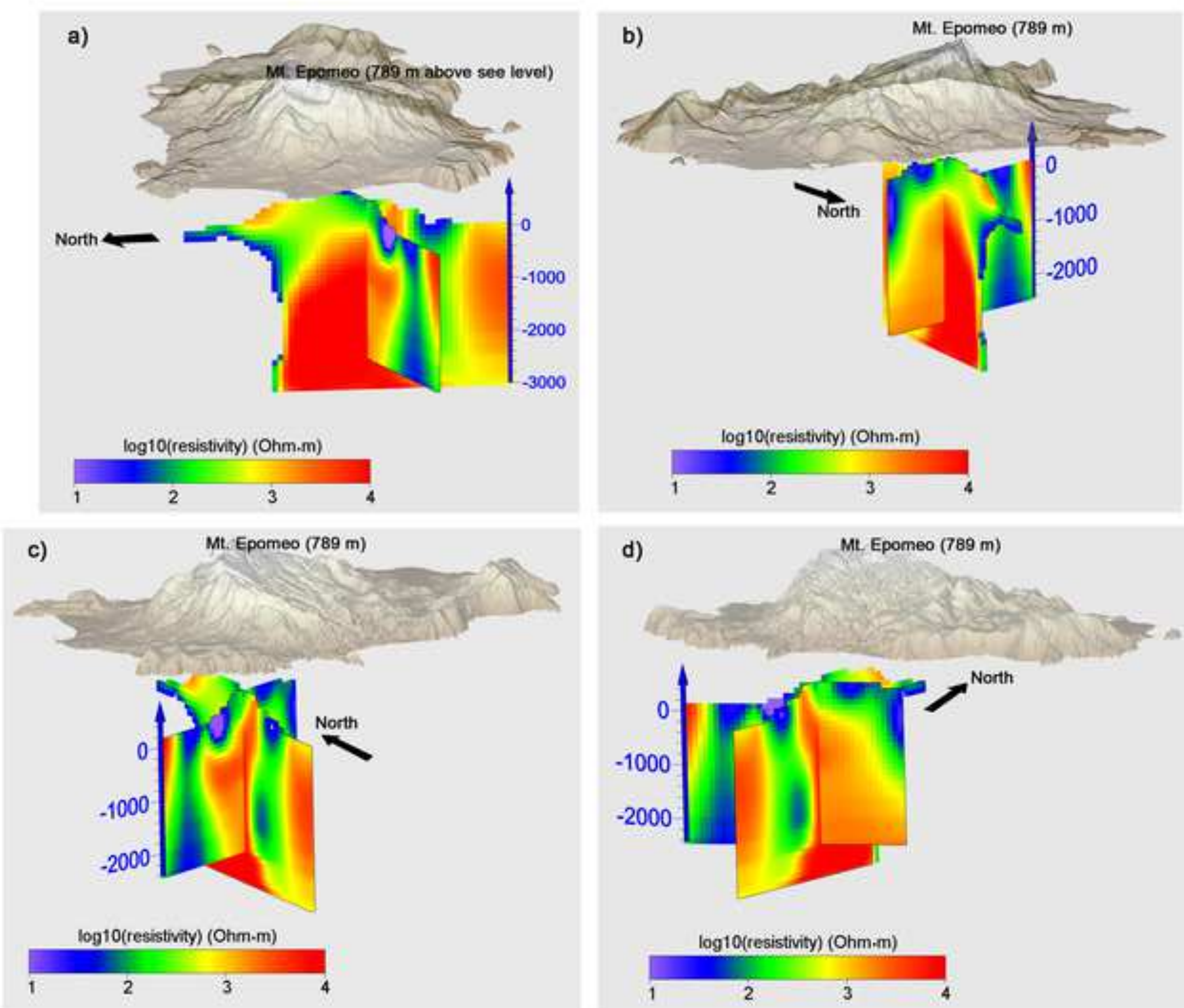
a)
Mt. Epomeo (789 m above see level)
North
0
-1000
-2000
-3000
log10(resistivity) (Ohm-m)
1
2
3
4
b)
Mt. Epomeo (789 m)
North
0
-1000
-2000
log10(resistivity) (Ohm-m)
1
2
3
4
c)
Mt. Epomeo (789 m)
North
0
-1000
-2000
log10(resistivity) (Ohm-m)
1
2
3
4
d)
Mt. Epomeo (789 m)
North
0
-1000
-2000
log10(resistivity) (Ohm-m)
1
2
3
4

Figure 9

Click here to download Figure Figure_9.tif

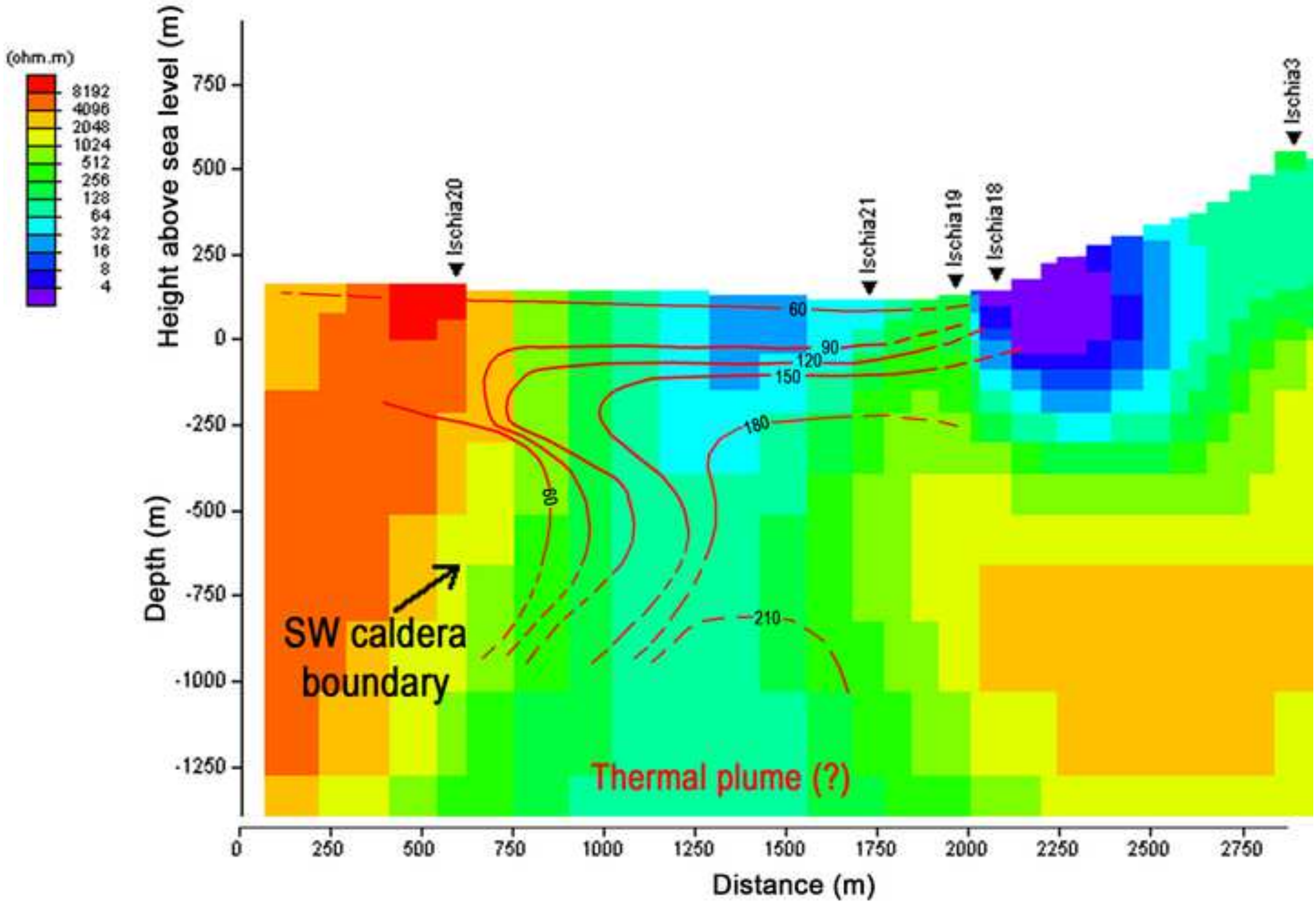

Figure 10

Click here to download Figure Figure_10.tif

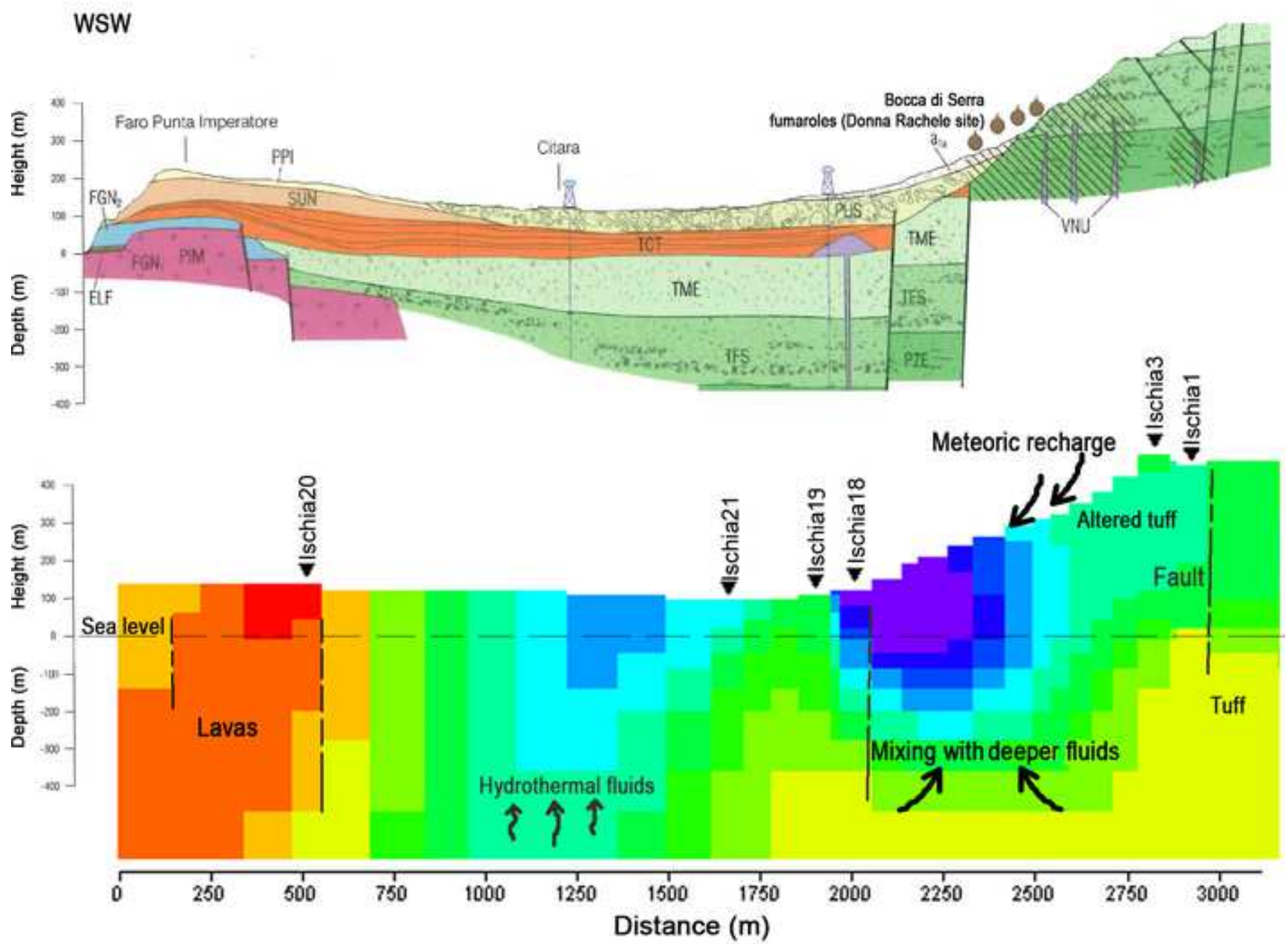

Figure 11a

Click here to download Figure Figure_11a.jpg

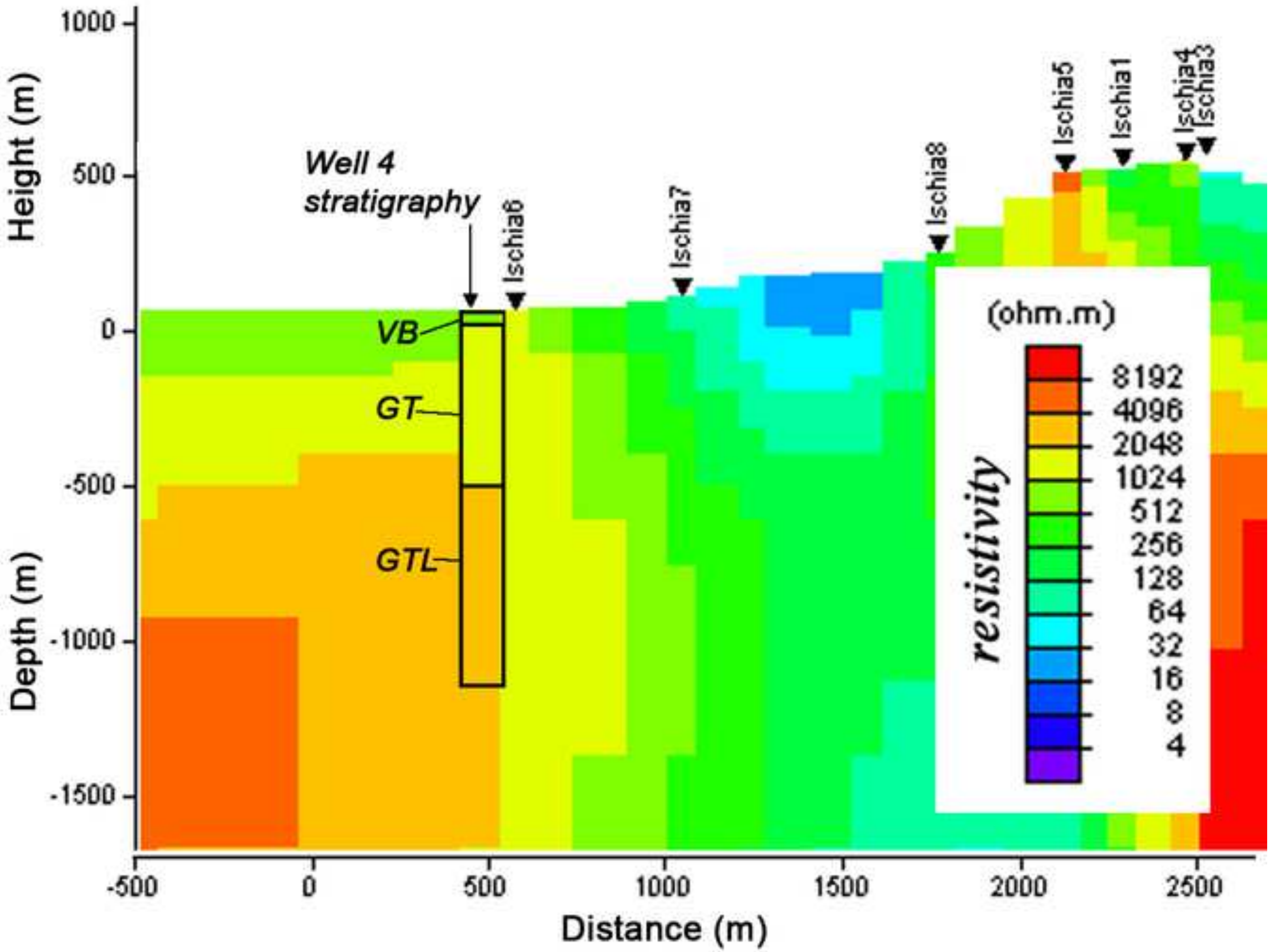

Figure 11b

Click here to download Figure Figure_11b.jpg

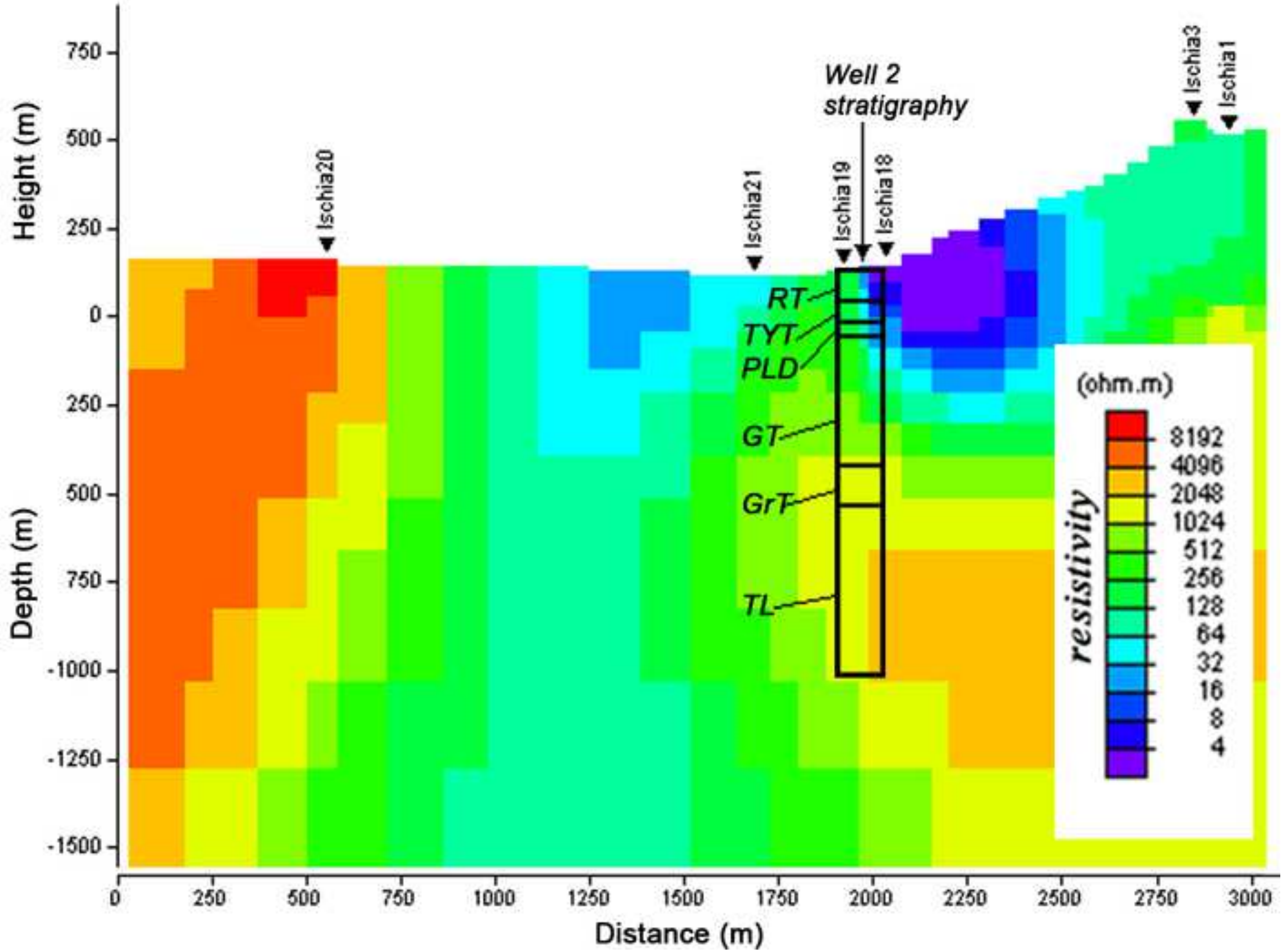

Magnetotelluric imaging of the resurgent caldera on the island of Ischia (Southern Italy): ~~the~~ inferences for its structure and activity ~~volcano-tectonics and dynamics~~.

Di Giuseppe, M. G., Troiano, A. and *Carlino, S.

Istituto Nazionale di Geofisica e Vulcanologia, Sezione di Napoli – Osservatorio Vesuviano (Italy)

*Corresponding author: stefano.carlino@ingv.it

Abstract

The island of Ischia (located in the Bay of Naples, Italy) represents a peculiar case of a well-exposed caldera that has experienced a large (>800 m) and rapid resurgence, accompanied by volcanic activity. What drives the resurgence of calderas is a crucial issue to investigate, because this process is associated with potential eruptions and high risk ~~for the~~to people living within and around ~~these~~ such large ~~volcanoes~~active volcanic systems. To improve the knowledge of volcano-tectonic processes affecting the caldera of Ischia ~~a new~~ electromagnetic imaging of the structures associated with ~~the~~ its resurgence was performed and integrated with ~~the~~ available geological information ~~available~~. A magnetotelluric (MT) survey of the island was carried out along two main profiles through the central-western sector, providing ~~the~~ an ~~first~~ electrical resistivity map to a depth of 3 km. These resistivity cross-sections ~~thus obtained~~ allowed us to identify the presence of a very shallow magmatic intrusion, possibly a laccolith, ~~to~~ at a depth of about 1 km, which was responsible for both the resurgence and the volcanic activity. Furthermore, the tectonic structures bordering the resurgent area and the occurrence of a large thermal anomaly in the western sector of the caldera also provided a signature in the resistivity cross-sections, with the magma intrusion producing ~~a vigorous~~ advection of hot fluids with high geothermal gradients (>150 °C km^{-1}) in the southern and western sectors. All of these data are fundamental for the assessment of the island's volcano-tectonic dynamics and their associated hazards. The ~~dynamics~~ structure and activity of the island have been ~~influenced~~ controlled by the process of resurgence ~~that is~~ associated with the arrival of new magma and the progressive intrusion of ~~the~~ a laccolith at a shallow~~er~~ depth. The reactivation of such a shallow system may imply imminent eruption ~~and~~ which would pose a major volcanic hazard.

Introduction

The resurgence of calderas was defined by Smith and Bailey (1969) as the process of uplift that usually occurs in the form of a structural dome that takes place after a caldera collapse. The uplift and bending of both the floor and roof of the caldera produce fracturing, faulting and,

~~furthermore~~thereby, enhance the development of permeability channels (Kennedy *et al*., 2012). While generation of ~~A~~ highly permeable network promotes the circulation of hot fluids, forming magmatic-hydrothermal systems (Hulen *et al*, 1987), ~~while~~ faulting and fracturing can also facilitate the migration of magma to the surface and, eventually, an eruption (Kilburn, 2003). Thus, resurgence plays a central role in the evolution of calderas, but the processes involved are still unclear, in particular with regard to the causes and the timing of ~~any~~ uplift. The most common process associated with the resurgence of calderas is the influx or intrusion of magma at various depths (Fridrich *et al*., 1991; Saunders, 2001; Jellinek and De Paolo, 2003; Kawakami *et al*., 2007). Other mechanisms contributing to ~~the~~ resurgence have been suggested, such as combination of regional detumescence and viscous rebound (Smith and Bailey, 1969; Marsh, 1984), volatile exolution and gas overpressure (Marsh, 1984), thermal expansion of the caldera fill (Kennedy and Stix, 2003) and the disturbance of geothermal fluids (Hurwitz *et al*., 2007; Chang *et al*., 2010, Troiano *et al*., 2011).

A crucial question is thus, what drives resurgence within calderas and (if magma is involved in this process), at what depths and of what volumes are the resultant intrusions? In the latter case, ~~(~~depending on the volcano-tectonic setting, the ~~dynamic~~ rate of uplift of the area and ~~the~~ magma~~'s~~ viscosity (~~;~~ Pollard and Johnson,1973; Smith and Bailey, 1969; Acocella *et al*., 2001; Carlino, 2012), the magmatic intrusion may evolve in a range of ways (e.g. to be emplaced as sills, dikes~~,~~ or laccoliths) producing a variable amount of uplift and a variety of resurgence structures (Paige, 1913; Orsi et al., 1991; Henry *et al*., 1997; Acocella *et al*., 2001 and references therein). The recognition of such differences is fundamental in the understanding ~~of~~ a caldera~~'s~~ ~~dynamic~~ structure and any associated hazard. As a result ~~and thus~~ the shallow and deep structures of calderas need to be better investigated through the application of effective geophysical methods. Among the geophysical surveys that can improve the knowledge of the deep structures of calderas, electrical resistivity mapping represents a reliable tool in the assessment of the buried structures in volcanic settings~~. This is supported by the relevant results obtained during many applications of electrical and electromagnetic geophysical methods, carried out in the last decade on both volcanic and tectonic structures~~ (Troiano *et al*., 2008; Troiano *et al*., 2009; Revil *et al*., 2010; Troiano *et al*., 2014; Di Giuseppe *et al*., 2015; Di Giuseppe *et al*., 2017b). In this work, a magnetotelluric (MT) survey was applied to the active volcanic caldera of Ischia, whose resurgence is thought to be associated to a sill intrusion, possibly developed in the form of a laccolith (Rittman, 1930; Sbrana *et al*., 2009; Carlino *et al*., 2006; Carlino, 2012 and references therein). The resurgence, which is estimated as at least 800 m (Vezzoli, 1988), was accompanied by volcanic activity and by the exhumation of the geothermal system (Sbrana et al., 2009), with the occurrence of a large diffuse heat flow and very high geothermal gradients (>180°C km^{-1}) in the shallow crust (Vezzoli, 1988; ~~Sbrana *et al*., 2009;~~ Carlino, 2012; Carlino *et al*., 2014; Carlino *et al*., 2015). ~~Beyond~~ Although a numbers of ~~specific~~ local geophysical investigations have been performed at Ischia (~~see Nunziata and Rapolla, 1987;~~ Di Napoli *et al*., 2009, 2011; Paoletti *et al*., 2013), a wider geophysical imaging of the island is not yet available. Such knowledge represents a crucial task in supporting ~~the~~ physical modeling (Rinaldi et al., 2011), to improve the understanding of the caldera's ~~dynamic~~structure and activity, and to assess the associated hazard on the island.

The MT survey was carried out in the central-western sector of the island. Through this survey, the electrical resistivity distribution was reconstructed in correspondence to two separate profiles (deployed in a N-S and a WSW-ENE direction respectively) (Figure 1). In this fashion two resistivity sections, respectively about 5 km and 3 km long, were obtained and interpreted ~~in order~~ to highlight the main geological features of the crust to a depth of 3 km including its thermal state, as well as location of fluid circulations and structural discontinuities ~~along~~ within both the collapsed and the uplifted areas. The results provide new insights ~~In particular, new evidences emerged~~ regarding both the thermal situation pertaining on the central-western sector of the island and the circulation of geothermal fluids. ~~The main finding was the~~We find presence of a crystalline structure (intrusive rocks with very low permeability) located beneath the Mount Epomeo block (Figure 1), which possibly represents the apical part of a degassed and cooling magmatic source (laccolith). The results obtained are important, not only because of the volcanic risk on the island (which has about 65,000 inhabitants and more than 1,500,000 visitors during the spring and summer months) but also for the volcano-tectonic evolution observed in many calderas worldwide, during resurgence ~~processes~~.

Main geological features of the island

The volcanic field of Ischia is part of the Phlegrean Volcanic District~~, which is the most important quaternary active volcanic area of the Mediterranean region~~ (Figure 1). The rim of ~~the~~ Ischia caldera, which formed after the Mount Epomeo Green Tuff (MEGT) eruption, 55 ka (Vezzoli, 1988), is not well documented, although there are ~~even though~~ a few signs of the rim ~~have been identified~~ in the NW, SW and SE sectors (Tibaldi and Vezzoli, 1998). The caldera, it would seem, has an elliptical shape with its major axis running ENE-WSW (Vezzoli, 1988). The ~~most~~ island's most important structural element is the ~~roughly~~ 4x4 km^2 resurgent block of Mount Epomeo (formed mainly by the MEGT), located in the centre of the caldera, which has been uplifted over the last 55 ka by a magmatic intrusion (Rittman, 1930; Sbrana *et al*., 2009). The edges of this block are marked by a system of sub-vertical faults with NW-SE, NE-SW and N-S strike (Vezzoli, 1988;

Acocella and Funiciello, 1999; Tibaldi and Vezzoli, 1998) (Figure 1). The existence of a possible magmatic intrusion, associated with the resurgence and post-caldera volcanic activity, was firstly inferred from gravity surveys by Carrara *et al*., (1983) and Nunziata and Rapolla (1987). More recently, the model of laccolith intrusion (proposed by Rittman, 1930) has been taken up again by interpreting stratigraphy, deep temperature, geochemical, magnetic, electric and gravity data (Carlino *et al*., 2006; Sbrana *et al*., 2009; Carlino 2012; Paoletti *et al*., 2013). Sbrana *et al*. (2009) provided a model of resurgence of the island by using an integrated analysis of melt and fluid inclusions, mineralogy and stable isotopic compositions of pumices, tuffs and syenitic xenoliths. The authors have shown thatIn this model the engine of the hydrothermal system of Ischia can be identified as being a in its shallow magmatic system (at around a depth of 2 km depth) that hosts hot trachytic magma. Accordingly, Carlino *et al*., (2006) and Carlino (2012) showed, through by the analytical modeling of the bending and fracturing of an elastic plate, that the resurgence of Mount Epomeo block may be associated to a sill-like intrusion which developed, during its later stages, into a laccolith, the top of which is located at a depth of about 2 km. Paoletti *et al*., (2013), using an integrated analysis of geophysical data, highlighted the presence of a possible magmatic intrusion, with a temperature below the Curie point, a density of about 2.4 g cm^{-3} and its top at a depth of about 2 km. The top of this magma body is slightly off-center, being decentred in the southwestern part of Ischia, where a fumarolic emissions are focused (Chiodini et al., 2004) robust geothermal circulation takes place. The total estimated uplift of the Mount Epomeo block, deduced from the present height of the marine deposits and eustatic variations, is 710 m in the southern sector and 920–970 m in the northern sector, with average rate of uplift ranging from 2.3 to 3.3 cm a^{-1} (Barra *et al*. 1992; Tibaldi and Vezzoli 2004; Carlino *et al*. 2006). During the resurgence over the last 28 ka, most of the eruptive centres have been aligned along the caldera structure (Vezzoli, 1988). Between 28 ka and 18 ka the volcanic activity migrated to the SW and SE sectors of the island (Fusi et al., 1990). while However, during the most recent period of activity, from 10 ka to 1302 A.D., the eruptive centres centers were have become clustered in the eastern and northern sector, with the emission of domes and lava flows (Vezzoli, 1988; Fusi *et al*., 1990; de Vita *et al*., 2010). The last eruption in the island took place in 1302 A.D. (de Vita et al., 2010), while the resurgence has probably been taking place actively since about 5ka (Vezzoli *et al*., 2009).

The circulation of underground hydrothermal fluids on the island is linked to its volcano-tectonic dynamicstructural setting, whose permeability is controlled which was characterized by the positioning relative location of lavas and pyroclastic deposits. FThe fluid circulation is thus correlated withto the occurrence and interlayering of different deposits, and mostly takes place at pathways of high permeability such as atthrough the fractures and faults inof welded tuffs and lavas and within the pores of unconsolidated pyroclastic deposits (Celico *et al*., 1999; Carlino *et al*., 2014). The shallow stratigraphy of the western sector (down to a depth of 1 km) has been inferred from ~~a range of~~ borehole measurements ~~s~~ (Penta and Conforto, 1951; see figure 1 for borehole locations). In the central zone of Mt. Epomeo and along its boundary ~~the~~ while coarse volcanic deposits ~~represent~~ form a ~~the~~ shallow permeable layer, ~~while~~ fractured tuffs, ~~and~~ lavas and marine clay deposits ~~characterize~~ make up ~~the~~ semi-permeable and impermeable layers, respectively. In the western area of the island the aquifer generally has a lower transmissivity than in the eastern sector (Celico *et al*., 1999). The effect of volcano-tectonic structures is noticeable above the main faults bordering Mt. Epomeo, where the shallow aquifers have been pushed ~~dislocated~~ upward in correspondence to the uplift of the block (Sbrana *et al*., 2009; Carlino *et al*., 2014). Along the western faults ~~are located the~~ hot springs are located about highly permeable path ways associated with high thermal energies ~~with larger capacity and greater thermal energy~~ (Chiodini *et al*., 2004) (Figure 1). Also inferred in the western sector is the occurrence of mixing processes between marine water and hydrothermal fluids, testified to by the high salinity of the fluids sampled ~~latter~~ close to the coast (Celico *et al*., 1999; Di Napoli *et al*., 2011). In the southwestern sector of the island the shallow resistivity model obtained by Di Napoli *et al*.~~,~~ (2011) highlights the presence of a zone of high conductivity, whose top is located at a depth of about 100 m and which is related to the superficial hydrothermal reservoir. Geothermal gradients of the island are typically very high, ranging in the hottest areas (south-western sector) from 180 °C k~~K~~m^{-1} to 200 °C k~~K~~m^{-1} (AGIP, 1987). These high gradients are associated with an efficient heat transport from the reservoir through an advection-dominated system (Carlino *et al*., 2012; Carlino *et al*., 2014). Taking into account ~~the above~~these gradients, the transition from a brittle to semi-brittle regime should take place at a depth of about 2-3 km (Carlino *et al*., 2014), while the depth of the brittle crust is possibly ~~higher~~ deeper in the north with respect to the southern sector (Carlino *et al*., 2006).

At present time the island is subject to slow subsidence, reflecting a gradual depressurization of the magmatic or hydrothermal system beneath Mount Epomeo (Sepe *et al*., 2007; De Martino *et al*., 2011).

MT data collection, analysis and inversion.

T~~In order t~~o characterize the first few ~~km~~ kilometers of the crust of the island of Ischia a magnetotelluric survey was performed. Magnetotellurics is an electromagnetic geophysical method for measuring the resistivity of the earth's interior by recording the natural electric (**E**) and magnetic (**H**) fields on the surface (Vozoff, 1991) as they vary over tme. In the present application, fluctuations of the orthogonal components of these fields ~~have been~~were recorded ~~in~~

~~correspondence to the~~at 20 measurement sites (see figure 1 for locations). Measurements were carried out using a Stratagem EH4 instrument, produced by Geometrics~~ and lasted as long as a few hours~~. Only the horizontal components of the **E** and **H** fields were recorded, neglecting the sampling of Hz which is usually considered as only providing limited additional information regarding the dimensionality of the Earth's local structure (Vozoff, 1991; Simpson and Bahr, 2005).

Once ~~the series of the~~data set of field fluctuations over time had been collected, the underground resistivity complexity was obtained as a rank-2 tensor, **Z**, correlating the two orthogonal pairs (E_x,E_y) and (H_x,H_y) at the E~~e~~arth's surface in the frequency-domain. This tensor is correlated with~~to~~ the MT apparent resistivity and phase curves, which compose the final dataset. To estimate such curves, the collected time series spectra have been estimated using a short ~~time~~ period Fourier transform performed over the ~~[~~$10^{-4} \sim 10^{1}$~~]~~ s ~~period~~ range. Such a period was examined ~~in order~~ to investigate the structures located across the first few ~~km~~ kilometers of depth below ground level. T~~In fact, t~~he investigated~~ive~~ depth of the electromagnetic waves depends on their capacity to penetrate into the Earth. This, in turn, is directly related to rock resistivity. In a uniform substrate the electric and magnetic fields weaken exponentially with depth, the more conductive the ~~earth~~rock, the lower the penetration. The depth at which the fields ~~had~~ decline~~d~~ to e^{-1} of their values at the surface is ~~called~~ termed the skin depth $\delta = (2\rho/\omega\mu)^{1/2} \approx 500(\rho/f)^{1/2}$ (in metres) where, ρ is the resistivity, f is the frequency of the wave, $\omega = 2\pi f$ and μ is the permeability. The latter is usually taken as being equal to μ_0 (free space permeability), except in highly magnetic materials. Frequency enters into the equations because the magnitudes of the induced telluric currents depend on the rate of change of the magnetic fields over time (Vozoff, 1991, Simpson and Bahr, 2005). ~~To record the electrical and magnetic fields fluctuations on the Earth's surface over such a time period, measurements were carried out through the use of Stratagem eh4® instruments, made by Geometrics, which were equipped with a couple of low frequency BF4 magnetometers. Only the horizontal components of the **E** and **H** fields were recorded, neglecting the sampling of Hz which is usually considered as only providing limited additional information regarding the dimensionality of the Earth's local structure (Vozoff, 1991; Simpson and Bahr, 2005).~~

After the application of short ~~time~~ period Fourier transform, data belonging to each ~~one~~ of the MT surveys were analyzed using the ~~robust~~ algorithm ~~presented in~~of Egbert and Booker (1986). This was used to avoid the distortion in the estimated MT curves, which might emerge from the time series due to the presence of anthropic noise, especially for surveys in urban~~ized~~ environments. This kind of algorithm has proven to be effective in the case of single station MT surveying (Egbert and Livelybrooks, 1996; Bai *et al*., 2001; Brasse *et al*., 2001; Pous *et al*., 2002). Its application in such a context was tested during the electromagnetic imaging of the nearby Campi Flegrei area (Troiano *et* *al*., 2014; Di Giuseppe *et al*., 2017a) ~~in order~~ to analyze ~~the~~ MT soundings. Its performance also proved to be adequate in the case of Ischia and the MT curves obtained do not appear affected by anomalous behaviour, such as a strong scattering of the points, strong oscillations or rises in the apparent resistivity, etc., that might signal the presence of coherent noise. Finally, the MT curves were analyzed using both MT-corrector® and Winglink® commercial software (Figure 2). ~~Some of the curves thus obtained are displayed in figure 2, as example of their general behavior.~~

~~Furthermore, o~~One of the first issues concerning magnetotelluric data is ~~so-called~~the *static-shift* (Jones, 1988). The data may suffer a sort of indetermination in the level of the apparent resistivity curves, due to the galvanic effects of shallower bodies. Such an issue, that does not affect the phase curves, was taken into account by carrying out Local Electrical Resistivity Tomographies (ERT). ERT, being based on a DC current source, does not suffer such issues and it is possible to use tomography of this kind to synthetically reconstruct the correct level of the MT apparent resistivity at high frequency. ~~In the following the dataset has been arranged considering t~~Two separate profile lines, which were oriented along N-S and the WSW-WNE transects were set up. These profiles, 5 km and 3 km long respectively, covered the central-western sector of the island (figure 1). For each of the two profiles the apparent resistivity and phase curves relative to both the TM (Transverse magnetic) and TE (Transverse electric) modes are shown in figure 3, under pseudosection form (Vozoff, 1991).

As an initial step, the MT data dimensionality was analyzed. ~~As is well known, t~~The introduced **Z**, which correlates the electric and magnetic fields on the Earth surface, presents peculiar characteristics in the case of 1D or 2D symmetries actually present in the data (Vozoff, 1991; Simpson and Bahr, 2005; Troiano *et al*., 2009) and several approaches exist in the literature to investigate this issue, namely the Wal method (Weaver *et al*., 2000), ~~the~~ phase tensor analysis method (Caldwell *et al*., 2004) and ~~the~~ Groom and Bailey's method (McNeice and Jones, 2001).

In the present case, ~~the~~ phase tensor analysis has been applied. This method, introduced by Caldwell~~,~~ *et al*. (2004) was ~~successively~~ well-described in Berdichevsky and Dmitrev (2010), where it is possible to retrieve details regarding the ~~overall~~ methodology, the definition of the phase tensor $[\Phi] = \begin{bmatrix}\Phi_{xx} & \Phi_{xy} \\ \Phi_{yx} & \Phi_{yy}\end{bmatrix}$ and all the derived quantities. Figure 4 reproduces the ~~behaviour~~behavior of the orientation of the phase tensor ellipse, i.e. the $\alpha_1 = \frac{1}{2} sin\left(\frac{\Phi_{xy}+\Phi_{yx}}{\Phi_{xx}+\Phi_{yy}}\right)$, ~~e.g.~~ ~~the α_1~~ angle, defined in Berdichevsky and Dmitrev (2010); it is also reproduced~~,~~ ~~and~~ the Caldwell-Bibby-Brown Skew angles, $skew_{CBB} = \frac{1}{2} arctan\left(\frac{\Phi_{xy}-\Phi_{yx}}{\Phi_{xx}+\Phi_{yy}}\right)$, for every survey, over four distinct frequency bands, respectively ~~centred~~centered on 0.9, 9, 90 and 900 Hz. In a model with the two-dimensional regional background, $skew_{CBB} = 0$ and the principal directions of the phase tensor coincide with the

α_1 angle. In the case of a 3D ~~the three-dimensonal~~ asymmetric regional background skew$_{CBB}$ $\neq$ 0. This angle represents a correction for the regional background asymmetry, which can be neglected if small, so that we can rely on the ~~resorting to the two-dimensional~~ 2D approximation of the regional background. As expected in a volcanic context, the skew$_{CBB}$ does not seem to present a ~~behaviour~~behavior adequate to support a 2D inversion ~~in the present case~~ and a different approach ha~~d~~s to be pursued. It is worth noting that this step is the basis on which to choose one of the possible strategies that might ~~turn out~~prove to be more satisfactory for the data inversion.

Despite the well-~~consolidated~~ tested 2D approach generally being thought of as the optimal to choose in terms of a compromise between the numerical complexities of the task and the affordability of the results, its incorrect application can lead to very misleading results and examples exist in literature where the differences originating from a 3D reinterpretation of previously analyzed MT data have led to models having very different implications (Booker, 2014). On the other hand, even if various 3D inversion codes have been proposed in the literature (Siripunvaraporn *et al*., 2005a; Kelbert *et al*., 2014) and if 3D inversion ~~is~~ has been actually developed in MT surveying (Rosenkjaer *et al*., 2015; Yang *et al*., 2015), such a procedure is still ~~turns out to be~~ not totally stable and requires a high number of sampling sites to be applied. In the Ischia survey work, the ~~logistical~~ morphological conditions limited the number of ~~surveys~~ sites and imposed the alignment of the sites along two crossed lines. This configuration has to be taken into account when the inversion strategy is questioned.

Many papers in the literature ~~concern~~ consider 3D ~~the three-dimensional~~ inversion of ~~two-dimensional~~ 2D profiles (e.g. Ledo *et al*., 2002; Siripunvaraporn *et al*., 2005b). ~~, which highlight~~These highlighte~~d~~ the limits of this approximation when the TM and TE apparent resistivity and phase are considered separately. Such a situation has also already been dealt with in Troiano *et al*. (2014), ~~which~~ who presented ~~the three-dimensional~~a 3D inversion of an electromagnetic survey carried out in the Campi Flegrei area. In this ~~last~~ case, the ~~one-dimensional~~1D inversion of the Z determinant has ~~proven~~ proved to be a useful tool to set up a strategy to interrogate the effects of ~~three-dimensional~~ buried structures in 3D based on ~~two-dimensional~~2D survey profiles. Such ~~quantities~~ considerations prove ~~turn out~~ to be particularly significant in volcanic environments (Ranganayaki, 1984; Pedersen and Engels, 2005; Troiano *et al*., 2014) and the resistivity model that can be obtained through this step, despite the strong limitation linked to the 1D approximation~~, may be an optimal starting model~~.

The likely indetermination related to the effects due to the eventual presence of lateral anomalies on the MT sections ~~have been~~were here ~~successively~~ taken into account through a 3D based ~~forward~~ trial-and-error procedure (Troiano et al., 2014). The latter ~~is~~ was carried out through the use of the subroutines of the WingLink® commercial code in order to estimate the apparent resistivity and phase curves. The subsoil was divided up into 76 ·~~x~~ 79 ·~~x~~ 36 cells, with dimensions ranging from 50 m (in the core of the modeled area) up to 1 km (in the external zones) and an objective function was ~~evaluated~~derived, based on the misfit between measured and reconstructed apparent resistivity and phases. This trial-and-error procedure begins with the resistivity model obtained using the 1D inversion of the Z determinant. A wide range of alternative models were then compared, taking as the most adequate that ~~the one~~ related to the lowest root mean square (r.m.s.). At the end of the procedure, an optimal model, corresponding to an r.m.s. less than seven~~a lower than 7 r.m.s. value~~, was selected. We note that ~~such a procedure is well founded in the literature and that~~ the r.m.s. value obtained here was compatible with ~~ones~~ those presented ~~in literature~~ for similar applications (e.g. Schwalenberg *et al.*, 2002; Abdul Azeez and Harinarayana, 2007; Rao *et al.*, 2007; Heise *et al.*, 2008; Arango *et al.*, 2009; Troiano *et al.*, 2009 and Troiano *et al.*, 2014).

An error threshold of 5% was considered for both the apparent resistivity and phase curves. More details for the data analysis and inversion procedures can be ~~retrieved~~ found in Troiano *et al.* (2008) and Troiano *et al.* (2014). The sections corresponding to the two ~~crossed~~ profiles of figure 1 are represented in figure 5 and figure 6, respectively. The main electrical anomalies have been labeled with capital letters and will be interpreted geologically in the following section.

Considering ~~At this point one last issue should be discussed concerning the description of the reliability of the results obtained from the MT data analysis. As an initial concern, taking into account the rule-of-thumb's for skin depth and considering~~ a mean electrical resistivity for the medium of about 100 Ωm, the maximum period of 10 s was found to be associated with a wave penetrating more than 15 km into the crust. The models of figure 5 and figure 6 resolve to a maximum depth of about 3 km.~~, which then prove to be completely determined~~. A ~~Apart from such empirical considerations, a~~ full sensitivity analysis was also carried out, following Schwalenberg *et al.* (2002). In figure 7 the sensitivity maps are reported, relative to the resistivity cross-sections of both figures 5 and ~~figure~~ 6. Sensitivity represents an estimate of the changes induced in the data by infinitesimal variations in the underground electrical resistivity. There is no~~t an~~ univocal threshold for the sensitivity required to indicate that a structure is well resolved, but the procedure presented in Troiano *et al.* (2008) and Troiano *et al.* (2009) supports the conclusion that both ~~the~~ our resistivity cross-sections are reliable. The consistency of the main bodies retrieved in the sections was further questioned by removing the anomaly from the model and recalculating the relative r.m.s. ~~The absence of significant changes in this parameter implies a lack of resolution of the analyzed zone. On other hand, s~~Significant r.m.s. variations with respect to the error thresholds ~~could~~ can be considered as an indicator that the investigated part of the model exhibits good resolution. For example, in the NS section ~~displayed in~~of figure 5, the resolution of the zones labeled as A, B1, B2 and C was tested. When the resistivity of the model was modified only ~~in the A~~ zone A, substituting the few tens of Ωm retrieved with the data inversion using the 200 Ωm identified in the surrounding area, a 13.4% change in the r.m.s. was obtained. This indicates that the A zone exhibits good resolution. Analogous results were obtained for ~~the remaining bodies~~all other zones.

Results

The resistivity imaging of the island of Ischia has allowed~~allows~~ us to recognize a number of sectors, down to a depth of 2-3 km, with resistivity anomalies that are ascribable to ~~the~~ distinctive processes and physical conditions of the hydrothermal system below the caldera~~the crust~~. From the S-N profile (Figure 5), moving from south to north, it is possible to highlight a relatively high~~er~~ resistivity zone ~~south~~ extending to station I6 (Ischia6) (this is zone A ~~with~~ where resistivity values of thousands of Ωm). There is then~~,~~ a lower resistivity channel (zone B, with a few tens to hundreds of Ωm) between the measurement stations I7 and I8, and a high resistivity zone (C) beneath the Mt. Epomeo resurgent block (several thousands Ωm at a depth below 1000 m, between stations I5 and I13). A~~ and a~~ further zone of lower resistivity (zone D) occurs on the northern coast (<50 Ωm).

Along the WSW-ENE profile (figure 6) a rapid change in resistivity (from several thousands of Ωm to a few tens of Ωm) is observed ~~in~~ to the WSW~~ zone~~. Beyond the anomaly beneath Mt. Epomeo (C1, a few thousand ~~of~~ Ωm), four other zones ~~were~~ can characterized. The first one is ~~A~~a channel with lower resistivity between the stations I20 and I21 (E) which is well developed down to the bottom of the profile (at a depth of 2.5 km). W~~ and w~~ithin ~~its~~ the interior of this channel, two lower resistivity zones (a few tens Ωm) appear: the first one (E1) is located at shallower depths, up to 500 m below the surface~~ level~~, and the second one (E2) develops from a depth of about 1500 m to the bottom of the profile. ~~Furthermore~~Finally, a roughly circular shallow area (F) with very low relative resistivity (less than ten Ωm) can be identified ~~uphill~~ ENE to station I18 (figure 6).

The agreement between the two resistivity cross-sections of figures 5 and ~~figure~~ 6 have been evaluated in f~~F~~igure 8, where a stereographic view of the retrieved anomalies is provided. In the area where the~~y~~ two profiles intersect ~~the~~ our magnetotelluric imaging detects a coherent resistive structure in correspondence to the Mt. Epomeo resurgent block.

Interpretation of the resistivity cross-sections

T~~As is well known, t~~he ~~peculiar~~ sensitivity of electrical resistivity to the presence of groundwater provides electrical and electromagnetic methods with a high detectability power ~~with respect to~~for resolving buried structures. However, once the presence of the electrical resistivity anomalies have been inferred~~,~~ in volcanic settings, the interpretation of the geophysical imaging remains inherently difficult. ~~As~~ Because the resistivity of rocks is generally affected by the water content, alteration (through their clay content and clay mineralogy), salinity of the pore water and temperature, the physical properties of porous rocks in geothermal and volcanic areas remain poorly known (e.g.~~. A digression regarding such issues can be read in~~ Revil *et al.*~~,~~ ~~(~~2002~~)~~, Revil *et al.* ~~(~~2017a~~)~~ and Revil *et al.* ~~(~~2017b)~~ and the references therein~~. ~~Summarizing their considerations, g~~Groundwater in volcanic settings flows within porous materials, which may ~~present~~ undergo a greater or lesser degree of alteration. This alteration is due to a chemical weathering of the minerals by the hot hydrothermal fluids, including hydration-dissolution processes of the volcanic glass and the formation of aluminosilicates such as ~~(~~clays and zeolites (Schön, 2015)~~)~~. Hydroelectric coupling in these porous rocks is influenced by the presence of these aluminosilicate minerals due to their role in blocking ~~as a result of their key position inside~~ the connected pore space. Electrical conductivity provides two contributions. The first is associated with conduction within the ~~bulk~~ pore water. The second ~~contribution, called~~is termed surface conductivity and~~,~~ is associated with conduction in the electrical double layer coating the surface of ~~the~~ grains (Berdichevsky and Dmitriev, 2010; Schön, 2015)~~)~~. Both of these processes ~~could~~ can bring about an increase in conductivit~~ies~~y and, using only resistivity data, it is not easy to separate surface from bulk conductivities at a given pore water conductivity. In our case, a numbers of ambiguities in the interpretation of our data were reduced by correlating the resistivity anomalies with data provided ~~by~~ from drilling~~s~~ (see figure 1 for locations), down to ~~a maximum~~ depth of 1150 m, and with previous geophysical and geochemical modeling of the island provided by Nunziata and Rapolla (1987), Chiodini et al. (2004), Paoletti et al. (2005), Di Napoli et al (2009), Di Napoli et al., (2011), Carlino (2012), Paoletti et al., (2013), Carlino et al. (2014).

The resistivity contrasts between ~~the~~ zones A, B, C and D ~~zones~~ of N-S profile (Figure 5) present a good correlation with the known volcano-tectonic features of the island, such as the boundary of caldera ~~collapse~~ and the Mount Epomeo resurgent block. In particular, the~~a~~ structural limit of the caldera is ~~perhaps~~ recognizable in the southern sector, close to the station I6. A normal fault, with a NW-SE strike affecting the south-western ~~uplift~~ sector of the resurgent block (see ~~also~~ figure 1 for fault location) (Vezzoli, 1988), ~~corresponds to~~coincides with the resistivity contrast between stations I5 and I8. In addition, north ~~to~~ of station I4, the resistivity variation pattern can be interpreted as the occurrence of minor faults facilitating the block uplift in the period since 33 ka

Formatted: Font: 12 pt

Formatted: Font: 12 pt

Formatted: Font: 12 pt

ago (Vezzoli *et al*., 2009). In the northern sector (figure 5) a low resistivity ~~surface~~zone, which deepens to about 700-800 meters down, ~~from~~ between the coast to the inner part of the island, is perhaps attributable to the interface between saline water and fresh water due to the latter's buoyancy. Between ~~the~~ measurement stations I7 and I8 a lower resistivity channel can be identified (B in figure 5). In particular, two major anomalies (B1 and B2) have been detected along this channel. The shallower one, B1, has a vertical extent of up to about 450 m b.s.l., while the deeper one, B2, develops from about 1100 m to 2500 m b.s.l. ~~According to the~~Following hydrothermal studies of the island (Di Napoli *et al*., 2009, 2011) and ~~from~~ drilling data (Penta and Conforto, 1951; Penta, 1963; AGIP, 1987), we ~~have~~ can interpret~~ed~~ the resistivity anomalies B1 and B2 as two aquifers, the former with a temperature of about 150°C, and the latter with a temperature of 250°C (Chiodini et al., 2004). These are~~,~~ formed by ~~a~~ mixing of liquid and~~+~~vapour (Chiodini et al., 2004). The lower levels of the aquifer B1 and the upper level of the aquifer B2 are in good agreement with the hydrothermal model proposed by Di Napoli *et al*.~~,~~ (2011). Along the WSW-ENE profile (Figure 6) two zones, E1 and E2, have been interpreted as two aquifers similar to those inferred along the N-S profile (B1 and B2). In accordance with the vertical tectonic movement of the island (resurgence), the top of ~~the~~ aquifer B2 (N-S profile of figure 5)~~, that~~ is closer to the uplift block and~~,~~ has been dislocated upwards with respect to the aquifer E2. The bottom of the aquifers are possibly sealed by argillfication processes which took place before ~~the~~ resurgence. Furthermore, as shown in Figure 9, the shape and location of the whole channel exhibiting low resistivity is possibly reconcilable with a thermal anomaly (a plume) associated with ~~a robust~~ advection of hydrothermal fluids. This is~~,~~ an interpretation also supported by ~~the~~ drill hole data ~~from drillings~~ and by the presence of ~~large~~ fumaroles and a hot-spring field (with temperatures up to 100°C), immediately north and west of ~~the~~ stations I20 and I21, respectively (Citara site, ~~see also~~ figure 1) (Penta and Conforto, 1951; AGIP, 1987; Chiodini *et al*., 2004; Di Napoli *et al*., 2011; Carlino *et al*., 2014). ~~As is well known, t~~The presence of such a thermal plume should leave a clear geophysical signature and the ~~carrying out of new~~futher surveys might allow it to be fully characterized (Jardani *et al*., 2008). One of the main features of the resistivity images is the occurrence of a high resistivity zone (>1000 Ωm) ~~identified~~ in both the N-S and WSW-ENE sections (see zones C and C1 in figures 5 and 6, respectively, as well as ~~and~~ figure 8). This anomaly is delimited ~~in the upper part~~ by the faults bordering the resurgent block. Considering the high heat flow and the elevated geothermal gradient of the area (Carlino *et al*., 2014), ~~which generally tends to lower the resistivity of rocks,~~ the relatively high resistivity anomaly (C and C1) can be ~~debated~~ explained in terms of ~~rock type and texture and their associated~~ permeability. ~~An initial remark is that the h~~High resistivity ~~is~~

~~possibly~~can be associated with a lower flow of hot hydrothermal fluids~~ into the rocks~~. This process, typical of many volcanic areas (Marsh, 1984), is related to the occurrence of crystalline rocks such as intrusive bodies with very low permeability (k) ~~or impermeable (e.g. k ranging~~which ranges from 10^{-17} to 10^{-21} m^2 for granite, for example~~)~~ (Brace, 1980). Such low permeabilities would~~These~~ inhibit the passage of fluids because the minimum permeability for volatiles to transfer into the shallow crust is 10^{-20} to 10^{-18} m^2, while for fluid transfer the figure is $\geq 10^{-16}$ m^2 (Ingebritsen *et al*., 2010). Furthermore, geochemical and isotopic investigations (Tedesco, 1996) have highlighted the presence of magmatic fluids~~ (with small crustal contamination)~~, which probably escape laterally from below to the magma body because they encounter a permeability barrier in a hugher ~~its upper and~~ more crystalline part. The presence of a shallow magmatic body (≈2 km in depth) beneath the Mount Epomeo resurgent structure, has~~d~~ already been inferred by other~~s~~ authors from interpretation of ~~ing~~ magnetic and gravity data (Nunziata and Rapolla, 1987; Paoletti *et al*, 2013 and references therein). For instance, the contemporary presence of a magnetic minimum and a gravimetric maximum (slightly decentred to the SW with respect to the centre of the island), might be explained by the existence of an intrusion or several intrusions and/or by partially melted zones to create pockets of crystal mush~~spots (mush)~~. This hypothesis is supported by the high temperature gradient measured in the central-western sector of the island (Penta and Conforto, 1951; Penta, 1954; Ippolito and Rapolla, 1982; Panichi *et al*., 1992; Paoletti *et al*., 2009). Furthermore, an undated intrusive rock was found at the bottom of the 1050 m deep ~~well~~drilling, located west of Mount Epomeo (well 2 in Figure 1) (Penta and Conforto, 1951; AGIP, 1987). Our findings seem to confirm the presence of such a shallow magmatic body~~, suggesting an even shallower one,~~ with a bulge penetrating up to about 1 km below the surface. Furthermore, taking into account the geothermal gradient of the island (about 200°C km^{-1}) (see Carlino *et al*., 2012, 2014 for details) the solidus temperature (onset of melting) may be encountered at a depth >3 km.

As a whole, we are confident that this magmatic body represents an intrusion and cannot be related to other ~~different~~ high resistivity structures, such as an uplifted ~~resistive~~ basement or unfractured rocks filling the caldera. Further observations supporting our statement include~~ the following~~: the high rate of resurgence of Mt. Epomeo, ~~clearly~~ which indicates~~ing~~ a magmatic process (injection) as driving mechanism (Tibaldi and Vezzoli, 2004; Sbrana *et al*., 2009) as driving mechanism; the observed pattern of deformation that can be associated with a shallow magmatic source with its top at about 2 km b.s.l. (Carlino, 2012)~~, with the top at about 2 km b.s.l~~; the observation that ~~arrival of~~ new trachybasaltic magma arrived in ~~into~~ the shallow magmatic system before the volcanic activity 28-18 ka (Civetta *et al*., 1991); the melt inclusion data that reveal that the ~~of~~ eruptive products of ~~(~~73-59 k~~ay)~~ ~~that were within~~came from a magmatic storage region located at a depth of about 2 km

(Sbrana *et al*., 2009) and, finally, the very high geothermal gradient and high temperature hydrothermal system, associated with the presence of a shallow magmatic body (Sbrana *et al*., 2009; Carlino *et al*., 2012, 2014).

The ~~structure of the~~ resistivity anomaly (figure 8) perhaps thus represents the apex of a laccolith (or alternatively a series of cone sheets) (Westerman *et al*., 2004) intruded into the shallow crust of the island (Rittman, 1930; Sbrana *et al*., 2009; Paoletti *et al*., 2013; Carlino *et al*., 2006; Carlino, 2012), ~~since at~~over the least 33 ka (Carlino, 2012 and references therein). Considering both the N-S and WSW-ENE profiles, the intrusion seems to have a branch that is elongated N~~-~~S in the western sector of Mt. Epomeo.

Finally, we can compare the WSW-ENE profile ~~has been compared~~ with the geology of the island (*Carta Geologica dell'isola d'Ischia*, CARG project), which in this sector is mainly constrained by the stratigraphy revealed from the drilling ~~stratigraphy~~ (figure 10). ~~From~~ As we seen in figure 10, ~~some correlations can be highlighted,~~ around ~~the~~ station I20~~, where~~ the resistivity anomaly (>2000 Ωm) corresponds to the Punta Imperatore lavas and to the eruptive ~~centre~~center of Campotese (see also figure 1). These lavas, dated to about 177 ka~~y~~ (Gillot *et al*., 1982), are dissected by faults that possibly do not involve the more recent, overlying, deposits and that are associated with ~~the~~ collapse of the caldera rim. ~~As already mentioned above, t~~The contrast in resistivity highlights the difference between the lower consolidated deposit of the inner caldera and the structural domes at the caldera rim. ~~Uphill~~ ENE to ~~the~~ station I18 a very low resistivity area coincides ~~is well matched~~ with the most important fumarole field of~~n~~ the island (Bocca di Serra, Donna Rachele fumaroles)~~, which we correlated to the argillification processes of the rocks as a result of hydrothermal alteration~~. The fumarole field covers about 0.80 km^2 (80 hectares), with emissions totaling ≈ 9 td^{-1} (volume) of CO_2 ~~rising~~ that rise along ~~from~~ a system of vertical faults (Chiodini *et al*., 2004). This system is perhaps partly fed by a relatively deep hydrothermal aquifer (about 600 m deep) (Chiodini *et al*., 2004), whose fluids take advantage of the~~along~~ the structural discontinuity (faults and fractures system) located at the boundary of the uplifted block. ~~It is~~We also ~~remarkable that we~~ note a coincidence ~~quite good agreement~~ between the variation in ~~the~~ lithology encountered in the stratigraphy of the ~~wells~~ drillings (~~wells~~ drillings ~~n.~~2 and ~~n.~~4, see figure 1 for location) (AGIP, 1987) and the variation in resistivity encountered in ~~the~~ our cross-sections (figure 11a, b). Finally, in order to assess the influence of the intrusion on the tilting of the Mt. Epomeo block (Acocella and Funiciello, 1999) we need to improve our measurements to get a wider 3D imaging, because the resistivity anomalies seem to have a complex shape that cannot be well constrained by 2D inversion.

Discussion

~~Among the worldwide caldera systems, the active volcanic island of Ischia represents a good case study to investigate the processes generating resurgence and associated volcanic activity.~~ Of the varying interpretations of the caldera resurgence process, the most common is that of magmatic intrusion which can evolve in a range of ways, from sills, to dikes or laccoliths~~, producing a variable amount of uplift and structures within the resurgent area~~ (Paige, 1913; Henry *et al*., 1997; Acocella *et al*., 2001 and references therein). This process is generally associated with the formation of well-developed geothermal systems (Hulen et al., 1987).

~~A~~ One ~~broader~~ implication of this study involves the mechanism producing ~~the~~ resurgence of calderas. As in the case of Ischia, the relatively high rate of uplift, which provides a strain rate of at least one order of magnitude larger than tectonic processes (Carlino, 2012), excludes a regional tectonic contribution~~e~~. The ~~large and~~ long-term rate of uplift makes it possible also to exclude any non-purely magmatic contribution to the resurgence, such as the oversaturation of volatile species in a shallow and crystallising magma body (Tait *et al*., 1989) or a fluid contribution (Hurwitz *et al*., 2007). These processes are typically associated to relative small-scale (metres) and short-term (months to~~,~~ years) disturbances and, as in the case of the contribution of fluids, a partial recovery~~ing~~ of the deformation occurring will take~~s~~ place (see, for instance, the example of Campi Flegrei caldera; Troiano *et al*., 2011 and references therein). The long-term resurgence of Ischia (from at least 33 ka to 5 ka) was punctuated by phases of quiescence (de Vita *et al*., 2010), which possibly corresponded to ~~the~~ periods of volcanic activity (Carlino *et al*., 2006). ~~, while~~ However a large~~r~~ proportion of the magma arriving in~~to~~ the shallow system (Civetta *et al*., 1991) has not been erupted, and merely contributes~~d~~ to the uplift of Mt. Epomeo (Carlino *et al*. 2012), forming a very shallow intrusion whose occurrence seems to be confirmed by resistivity data. This behaviour ~~that, for instance,~~ is different when compared to that of the nearby Campi Flegrei caldera, (where some caldera sectors were uplifted by less than 100 m, while larger eruptions occurred). It~~,~~ is instead similar to ~~other volcanoes, as observed for~~ the Grizzly Peak caldera (Colorado) (Fridrich et al., 1991) and ~~for the volcanic island of~~ Pantelleria (Southern Italy) (Orsi et al., 1991). In ~~the above~~these cases, the rheology of the shallow magma sources and the response of the surrounding rock walls to the stress induced by the pressure of the magma possibly control the different evolutions of caldera resurgence ~~(total uplift vs. erupted volumes)~~. For instance, the temperature of the intruded magma and of the surrounding rock, ~~walls~~ together with the injection rate, strongly affect the behaviour of the system (Jellinek and DePaolo, 2003). Large geothermal gradients and low magma injection rates enhance creep processes instead of catastrophic failure, increasing the accretion of magma at depth and inhibiting eruptions (Jellinek and DePaolo, 2003). Overall, when the magma is the primary source of the resurgence of calderas, it is crucial to estimate its volume, thermal state and thermal history (Cooper and Kent, 2014), while the rheology of the magma itself and of the surrounding rock walls is critical in the evolution of the resurgence (Carlino and Somma, 2010). For the island of Ischia, if we assume a roughly radial symmetry of the resistivity anomaly associated with the magma intrusion (about 2 km in radius and 2 km in vertical extension), at least for the crust down to 3 km, that we obtain get a magma volume of about 6 km^3. If this has been gathering since 33ka (Tibaldi and Vezzoli, 1998), then the accumulation rate is about $1.8 \cdot 10^{-4}$ km^3 a^{-1}.This possibly represents a lower limit of the volume of magma (and the magma rate) intruded into the shallow crust, which, in its present state (having been gathering over 33ka), is not likely to prove eruptible due to its thermal condition. That is (the magma is will be highly degassed and the maximum temperature is possibly ≤ 600°C (and is below the melting point; see also Carlino et al., 2014).

Conclusions

The Our magnetotelluric survey carried out in the southern and western sector of the island of Ischia, detected several electrical resistivity anomalies, up down to a depth of 3 km. The interpretation of the resistivity cross-sections and the comparison with previous other geological, geophysical and geochemical studies data provide allow the following main findingsconclusions and inferenes:

- a good correlation, according to data in the literature (Schön, 2015), has been observed between the known geological information (stratigraphy inferred from drilling data) and the range of variation in the area's resistivity anomalies (see figure 11a, b).
- a large thermal anomaly has been inferred found in the southern and western sector of the island and is associated with a sustained zone of heat advection of and circulation of hydrothermal fluids (Figure 5 and 6). The presence of two major hot aquifers, previously hypothesized by geochemical studies (Chiodini *et al*., 2004, Di Napoli *et al*., 2011), has also been definitely locatedlized in the southwestern sector of the caldera. The aquifers are foundreside at different depths, with the depths being controlled bydepending on the vertical tectonic movements, which have affected caused deformation of the resurgent block of Mt. Epomeo for over at least the last 33 ka (Vezzoli, 1988)y. The top of the deeper aquifers, feeding the main south-western fumarole fields, and are located at a depth of about 1000 m to 1500 m, respectively.

Formatted: Superscript

Formatted: Superscript

Formatted: Superscript

- a large resistivity anomaly is located below the resurgent structure of Mt. Epomeo.~~, along both the N-S and WSW-ENE profiles.~~ It is interpreted as the apical part of a crystalline (and very low permeability) magmatic body intruded below the central part of the island (and slightly dislocated towards the south-west) and whose apex reaches a depth of about 1 km b.s.l. ~~(in the central-western part) and the bulk body of which is~~This body is bounded by an abrupt resistivity drop corresponding to the faults ~~close~~ around to the resurgent block of Mt. Epomeo.
- we ~~suppose~~ propose that this high resistivity body is associated with the laccolith of Ischia (Rittman, 1930; Sbrana *et al*., 2009; Carlino, 2012), which produced the bending, fracturing and faulting of the overlying crust, and which witnessed~~a further~~ magma intrusion during the ~~final~~ most recent stage of the resurgence (5 ka) (Civetta *et al*., 1991; Vezzoli *et al*., 2009). As result, the uplifted block h~~w~~as been broken up into minor blocks, with the underlying laccolith possibly developing as a complex structure.~~, formed by various protrusions on its apex~~. This laccolith is the engine of the robust geothermal system of the island, and -to be consistent with a high resistivity - is likely dominated by a highly crystalline mush~~.~~
- ~~finally, the finding~~the existence of such a shallow magma body is critical in terms of volcanic hazard assessment~~ on the island~~. The volcanism of ~~the island~~ Ischia seems, in fact, to be strictly correlated to the resurgence process that, in turn, is reliant on the dynamics of the laccolith (Carlino, 2012). A renewal of ~~the~~ resurgence ~~is thus~~will be related to ~~the~~ reactivation of the laccolith ~~(e.g. the~~by arrival of new magma) (Civetta *et al*., 1991).~~,~~This ~~which~~ may possibly produce a large disturbance of the geothermal system at a depth of between 1 km and 2 km. A reactivation of such a shallow magmatic system may imply imminent eruption and ~~a~~ would pose high volcanic hazard (e.g.Cooper & Kent, 2014); certainly it would cause hydrothermal emissions to evolve towards magmatic (Vaselli et al., 2010)~~.~~.

Figures captions

Figure 1. Structural and geological map of Ischia Island (after Di Napoli *et al*., 2011). ~~Indicated are t~~The MT measurement stations along the N-S profile are given as ~~(~~blue points~~)~~; the MT measurement stations along the WSW-ENE profile are ~~(~~green points; the blue-green points are ~~the~~ stations belonging to both the profiles~~)~~; Drilling sites are given as ~~the geological section A-A' used~~

in the text; the deep wells on the island (red points numbered from 1 to 5). The shaded grey circular area indicates the resurgence zone and black lines are mapped faults (Di Napoli et al. 2011). The dotted red lines indicate the resistivity section profiles.

Figure 2. Three examples of apparent resistivity and phase diagrams pertaining to the Ischia MT survey work.

Figure 3. (a) NS S-N Magnetotelluric profiles of apparent resistivity (above) and phase (below) pseudosections relative to the TM mode. (b) NS S-N Magnetotelluric profiles of apparent resistivity (above) and phase (below) pseudosections relative to the TE mode. (c) WSW-ENE mMagnetotelluric profiles of apparent resistivity (above) and phase (below) pseudosections relative to the TM mode. (d) WSW-ENE Magnetotelluric profiles of apparent resistivity (above) and phase (below) pseudosections relative to the TE mode (see text for details).

Figure 4. Results of the data dimensional analysis carried on the Ischia MT dataset using the phase tensor approach. The data have been divided up into four contiguous frequency bands, respectively centered on 0.,9 9, 90 and 900 Hz. The phase- tensor ellipse orientation (in degrees) (e.g. the α_1 angle defined in Berdichevsky and Dmitrev, 2010) and the Caldwell-Bibby-Brown Skew angles are reportedgiven, for each MT survey, respectively in (panel a) and (panel b), respectively.

Figure 5. S-N resistivity profile obtained from the inversion of the MT survey (panel b). It is possible to recognize different resistivity contrasts associated with volcano-tectonics and geothermal features of the island. Dotted lines are the faults associated with the caldera boundary and to the dislocation of the resurgent block (see text for details). It is also reported (toppanel a) the topographic profile along the section.

Figure 6. WSW-ENE resistivity profile obtained from the inversion of the MT survey (panel b). The resistivity anomaliesy (indicated marked as E, E1 and E2) has been associatedis coincident with a thermal plume producing high geothermal gradients and very high temperatures (~100°C) at the surface (see also figure 7Carlino et al., 2014). It is also reported (toppanel a)) the topographic profile along the section.

Figure 7. Sensitivity cross-sections relative to the resistivity models shown in figure 5 (NS S-N profile, above) and figure 6 (WSW-ENE profile, below).

Figure 8. Topography in shaded relief of Ischia draped over the DEM (INGV web-GIS source), perspective views from W (a), NE (b), SW (c), S (d). Beneath each are the resistivity data for the two profiles so as to set in context the variations we record with depth, as well as distance from Mt. Epomeo."Summarizing figure for resistivity profiles from different point of views. It is possible to infer the shape of the intrusion which exhibits a complex structure formed by very shallow protrusions.

Figure 9. Magnification of the central part of the WSW-ENE profile compared with the geotherms (after Carlino et al., 2014) Comparison of a detail of figure 6 (WSW-ENE resistivity profile) with

~~the isotherms obtained from the temperatures measured inside the wells down to a depth of 1000m (see figure 1 for well locations)~~

Figure 10. Comparison of the shallower part of WSE-ENE resistivity profile with a geological section of the island (from *Carta Geologica dell'Isola d'Ischia*, CARG project). *Legend: PZE =~~:~~ Pizzone Tuffs (~61 ka); TFS =~~:~~ Frassitelli Tuffs (~62 ka);VNU =~~:~~ dike and tabular intrusions~~-~~; TME =~~:~~ Mount Epomeo Green Tuff (~55 ka); PIM-FGN =~~:~~ Punta Imperatore ancient lavas (~117 ka); ELF =~~:~~ Elephant pyroclastic deposits; TCT =~~:~~ Citara Tuffs (~45 Ka);SUN =~~:~~ debris and mud flow deposits; PPI =~~:~~ Punta Imperatore pyroclastic deposits (~ 18 ka); PUS =~~:~~ Punta Soccorso debris avalanche; a_{1a} = alluvial deposits. (from CARG project)*

Formatted: Subscript

Figure 11 (a, b). ~~Detail~~ Magnification of the sections given in~~of~~ figures 5 and 6 with the position od drill sites ~~and stratigraphy of well numbers~~ 2 and 4 (see figure 1 for location) from which stratigraphic data are taken. ~~The comparison has been carried out to correlate the variation in the resistivity with the different layering of buried rocks.~~ Legend: (~~well~~ drill n. 4) VB = Volcanic Breccia; GT = Green Tuff; GTL = Green Tuff interlayered with trachytic lava. (~~well~~ drill n. 2) RT = Reworked Tuffs and Alluvium; TYT = Trachytic Yellow Tuffs; PLD = Pyroclastic and Lava deposits; GrT = Green Tuff; TL = Trachytic lava

Acknowledgements: This work was carried out in the framework of the INGV-DPC Research Agreement 2012–2021 "All. A". ~~This paper does not necessarily represent DPC official opinion and policies.~~ We are grateful to the Associate Editor, V. ~~Acocella~~ Acocella, the Executive Editor, A. Harris, and to the Referees, J. Stix and A. Revil, for their helpful comments that have greatly improved the quality of the work.

References

Abdul Azeez K, Harinarayana, T (2007) Magnetotelluric evidence of potential geothermal resource in Puga, Ladakh, NW Himalaya. Curr. Sci., 93, 323–329.

Acocella V, & Funiciello R (1999) The interaction between regional and local tectonics during resurgent doming: the case of the island of Ischia, Italy. Journal of Volcanology and Geothermal Research, 88(1), 109-123.

Acocella V, Cifelli F, & Funiciello R (2001) The control of overburden thickness on resurgent domes: insights from analogue models. Journal of Volcanology and Geothermal Research, 111(1), 137-153.

AGIP (1987) Geologia e geofisica del sistema geotermico dei Campi Flegrei, Technical report, Settore Esplor e Ric Geoterm-Metodol per l'Esplor Geotermica, San Donato Milanese Italy, pp 1–23

Arango C, Marcuello A, Ledo J, Queralt P (2009) 3D magnetotelluric characterization of the geothermal anomaly in the Llucmajor aquifer system (Majorca, Spain). J. Appl. Geophys., 68 (4), 479–488.

Bai, D., Meju, M. A., & Liao, Z. (2001). Magnetotelluric images of deep crustal structure of the Rehai geothermal field near Tengchong, southern China. Geophysical Journal International, 147(3), 677-687.

Barra, D., Cinque, A., Italiano, A., & Scorziello, R. (1992). Il Pleistocene superiore marino di Ischia: paleoecologia e rapporti con l’evoluzione tettonica recente. Studi geologici Camerti, 1(special issue), 231-243 (*in italian*)

Brace W F (1980, October) Permeability of crystalline and argillaceous rocks. In International Journal of Rock Mechanics and Mining Sciences & Geomechanics Abstracts (Vol. 17, No. 5, pp. 241-251). Pergamon.

Berdichevsky, M. N., & Dmitriev, V. I. (2010). Models and methods of magnetotellurics. Springer Science & Business Media.

Booker, J. R. (2014). The magnetotelluric phase tensor: a critical review. Surveys in Geophysics, 35(1), 7-40.

Brasse, H., & Soyer, W. (2001). A magnetotelluric study in the Southern Chilean Andes. Geophysical Research Letters, 28(19), 3757-3760.

Caldwell T, Grant H, Bibby M, Brown C (2004) The magnetotelluric phase tensor. Geophys. J. Int. 158, 457–469.

Carlino S, Cubellis E, Luongo G, Obrizzo F (2006). On the mechanics of caldera resurgence of Ischia Island (southern Italy). Geological Society, London, Special Publications, 269(1), 181-193.

Carlino S, and Somma R (2010) Eruptive versus non-eruptive behaviour of large calderas: the example of Campi Flegrei caldera (southern Italy), Bulletin of Volcanology, 72(7), 871–886

Carlino S (2012) The process of resurgence for Ischia Island (southern Italy) since 55 ka: the laccolith model and implications for eruption forecasting. Bulletin of V~~v~~olcanology, 74(5), 947-961.

Carlino S, Somma R, Troise C, De Natale G (2012) The geothermal exploration of Campanian volcanoes: Historical review and future development. Renewable and Sustainable Energy Reviews, 16(1), 1004-1030.

Carlino S, Somma R, Troiano A, Di Giuseppe M G, Troise C, De Natale G (2014). The geothermal system of Ischia Island (southern Italy): critical review and sustainability analysis of geothermal resource for electricity generation. Renewable Energy, 62, 177-196.

Carlino S, Somma R, Troiano A, Di Giuseppe M G, Troise C, & De Natale G (2015) Geothermal Investigations of Active Volcanoes: The Example of Ischia Island and Campi Flegrei Caldera (Southern Italy). In Engineering Geology for Society and Territory-Volume 1 (pp. 369-372). Springer, Cham.

Carrara E, Pinna E, & Rapolla A (1983) Indagini geofisiche nelle aree vulcaniche italiane di interesse geotermico. Atti Accademia Pontaniana, Nuova Serie, XXXI, 299–314.

CARG project (2011) Carta Geologica dell’Isola d’Ischia ~~(2011) Progetto CARG~~, Regione Campania.

Celico P, Stanzione D, Esposito L, Formica F, Piscopo V, De Rosa B M (1999) La complessità idrogeologica di un'area vulcanica attiva; l'Isola d'Ischia (Napoli, Campania). Bollettino della Società Geologica Italiana, 118(3), 485-504.

Chang W L, Smith R B, Farrell J, & Puskas C M (2010) An extraordinary episode of Yellowstone caldera uplift, 2004–2010, from GPS and InSAR observations. Geophysical Research Letters, 37(23).

Chiodini G, Avino R, Brombach T, Caliro S, Cardellini C, de Vita S,.... & Ventura G (2004) Fumarolic and diffuse soil degassing west of Mount Epomeo, Ischia, Italy. Journal of Volcanology and Geothermal Research, 133(1), 291-309.

Civetta L, Gallo G, Orsi G (1991) Sr-and Nd-isotope and trace-element constraints on the chemical evolution of the magmatic system of Ischia (Italy) in the last 55 ka. Journal of Volcanology and Geothermal Research, 46(3), 213-230.

Cooper K M, & Kent A J (2014). Rapid remobilization of magmatic crystals kept in cold storage. Nature, 506(7489), 480.

de Vita S, Sansivero F, Orsi G, Marotta E, Piochi M (2010) Volcanological and structural evolution of the Ischia resurgent caldera (Italy) over the past 10 ky. Geological Society of America Special Papers, 464, 193-239.

De Martino, Tammaro U, ObrizzoF, Sepe V, Brandi G, D'Alessandro, DolceM, Pingue F (2011) La Rete GPS dell'isola di Ischia: deformazioni del suolo in un'area vulcanica attiva (1998-2010). Quaderni di Geofisica, n.92.

Di Giuseppe M G, Troiano A, Fedele A, Caputo T, Patella D, Troise C, De Natale G (2015) Electrical resistivity tomography imaging of the near-surface structure of the Solfatara Crater, Campi Flegrei (Naples, Italy). Bulletin of Volcanology, 77(4), 27.

Di Giuseppe, M. G., Troiano, A., & Patella, D. (2017a). Separation of plain wave and near field contributions in Magnetotelluric time series: A useful criterion emerged during the Campi Flegrei (Italy) prospecting. Journal of Applied Geophysics. doi: 10.1016/j.jappgeo.2017.03.019.

Di Giuseppe M G, Troiano A, Di Vito M A, Somma R, & Matano F (2017b) Definition of small-scale volcanic structures by Electrical Resistivity Tomography: the Trentaremi cone, an example from the Campi Flegrei Caldera (Italy). Annals of Geophysics, 60(5), 0552.

Di Giuseppe M G, Troiano A, Patella D, Piochi M, & Carlino S (2017c). A geophysical k-means cluster analysis of the Solfatara-Pisciarelli volcano-geothermal system, Campi Flegrei (Naples, Italy). Journal of Applied Geophysics.

Di Napoli R, Aiuppa A, Bellomo S, Brusca L, D'Alessandro W, Gagliano Candela E, Longo M, Pecoraino G, Valenza M (2009) A model for Ischia hydrothermal system: evidences from the chemistry of thermal groundwaters. Journal of Volcanology and Geothermal Research, 186(3), 133-159.

Di Napoli R, Martorana R, Orsi G, Aiuppa A, Camarda M, De Gregorio Gagliano Candela E, Luzio D, Messina N, Pecoraino G, Bitetto M, de Vita S, Valenza M (2011) The structure of a hydrothermal system from an integrated geochemical, geophysical, and geological approach: The Ischia Island case study. Geochemistry, Geophysics, Geosystems, 12(7).

Egbert G D, Booker J R (1986) Robust estimation of geomagnetic transfer functions. Geophysical Journal International, 87(1), 173-194.

Egbert, G. D., & Livelybrooks, D. W. (1996). Single station magnetotelluric impedance estimation: Coherence weighting and the regression M-estimate. Geophysics, 61(4), 964-970.

Fridrich CJ, Smith RP, DeWitt E, McKee EH (1991) Structural, eruptive, and intrusive evolution of the Grizzly Peak caldera, Sawatch Range, Colorado. Geol Soc Am Bull 103 : 1160–1177.

Fusi N, Tibaldi A, Vezzoli L (1990) Vulcanismo, risorgenza calderica e relazioni con la tettonica regionale nell'isola d'Ischia. Memorie della Società Geologica Italiana, 45, 971-980.

Gillot P Y, Chiesa, S, Pasquare G, & Vezzoli L (1982). < 33,000-yr K–Ar dating of the volcano–tectonic horst of the Isle of Ischia, Gulf of Naples. Nature, 299(5880), 242-245.

Heise W, Caldwell T G, Bibby H M, Bannister S C (2008) Three-dimensional modelling of magnetotelluric data from the Rotokawa geothermal field, Taupo Volcanic Zone, New Zealand. Geophys. J. Int., 173 (2), 740–750.

Henry, C D, Kunk, M J, Muehlberger, W R, Mcintosh, W C (1997) Igneous evolution of a complex laccolith–caldera, the Solitario, Trans- Pecos. Texas: implications for calderas and subjacent plutons. GSA Bulletin, 109, 1036–1054.

Hulen J B, Nielson D L, Goff F, Gardner J N, & Charles R W (1987) Molybdenum mineralization in an active geothermal system, Valles caldera, New Mexico. Geology, 15(8), 748-752.

Hurwitz S, Christiansen L B, & Hsieh P A (2007) Hydrothermal fluid flow and deformation in large calderas: Inferences from numerical simulations. Journal of Geophysical Research: Solid Earth, 112(B2).

Ingebritsen S E, Geiger S, Hurwitz S, Driesner T (2010). Numerical simulation of magmatic hydrothermal systems. Reviews of Geophysics, 48(1).

Ippolito F, Rapolla A, (1982) L'energia geotermica in Campania. Fonti Energetiche Alternative, Fondazione Politecnica per il Mezzogiorno. Franco Angeli Ed., Milan, pp. 57–106 (in Italian).

Jardani A, Revil A. Bolève A. & Dupont J P (2008), 3D inversion of self-potential data used to constrain the pattern of ground water flow in geothermal fields, Journal of Geophysical Research, 113, B09204, doi: 10.1029/2007JB005302.

Jellinek A M, & DePaolo D J (2003) A model for the origin of large silicic magma chambers: precursors of caldera-forming eruptions. Bulletin of Volcanology, 65(5), 363-381.

Jones, A G (1988) Static shift of magnetotelluric data and its removal in a sedimentary basin environment. Geophysics, 53(7), 967-978.

Kawakami Y, Hoshi H, & Yamaguchi Y (2007) Mechanism of caldera collapse and resurgence: observations from the northern part of the Kumano acidic rocks, Kii peninsula, southwest Japan. Journal of Volcanology and Geothermal Research, 167(1), 263-281.

Kelbert A, Meqbel N, Egbert G D, & Tandon K (2014) ModEM: a modular system for inversion of electromagnetic geophysical data. Computers & Geosciences, 66, 40-53.

Kennedy B, & Stix J (2007) Magmatic processes associated with caldera collapse at Ossipee ring dyke, New Hampshire. Geological Society of America Bulletin, 119(1-2), 3-17.

Kennedy B, Wilcock J, & Stix J (2012) Caldera resurgence during magma replenishment and rejuvenation at Valles and Lake City calderas. Bulletin of volcanology, 74(8), 1833-1847.

Kilburn C R (2003) Multiscale fracturing as a key to forecasting volcanic eruptions. Journal of Volcanology and Geothermal Research, 125(3), 271-289.

Ledo J, Queralt P, Martí A, & Jones A G (2002) Two-dimensional interpretation of three-dimensional magnetotelluric data: an example of limitations and resolution. Geophysical Journal International, 150(1), 127-139.

Marsh B D (1984) On the mechanics of caldera resurgence. Journal of Geophysical Research: Solid Earth, 89(B10), 8245-8251.

McNeice G W, Jones A G (2001) Multisite, multifrequency tensor decomposition of magnetotelluric data. Geophysics 66, 158–173.

Nunziata C, Rapolla A (1987) A gravity and magnetic study of the volcanic island of Ischia, Naples (Italy). Journal of volcanology and geothermal research, 31(3-4), 333-344.

G. Orsi, G. Gallo, A. Zanchi (1991) Simple-shearing block resurgence in caldera depressions. A model from Pantelleria and Ischia J. Volcanol. Geotherm. Res., 47, pp. 1-11

Paige, S (1913) The bearing of progressive increase of viscosity during intrusion on the form of laccoliths. The Journal of Geology, 21(6), 541-549.

Panichi C, Bolognesi L, Ghiara M R, Noto P, Stanzione D(1992) Geothermal assessment of the island of Ischia (southern Italy) from isotopic and chemical composition of the delivered fluids. J. Volcanol. Geotherm. Res. 49, 329–348.

Paoletti V, Di Maio R, Cella F, Florio G, Motschka K, Roberti N, ... & Rapolla A (2009) The Ischia volcanic island (Southern Italy): Inferences from potential field data interpretation. *Journal of Volcanology and Geothermal Research*, *179*(1), 69-86.

Paoletti V, D'Antonio M, & Rapolla A (2013) The structural setting of the Ischia Island (Phlegrean Volcanic District, Southern Italy): inferences from geophysics and geochemistry. Journal of Volcanology and Geothermal Research, 249, 155-173.

Pedersen L B, & Engels M (2005). Routine 2D inversion of magnetotelluric data using the determinant of the impedance tensor. Geophysics, 70(2), G33-G41.

Penta F (1954) Ricerche e studi sui fenomeni esalativi-idrotermali e il problema delle forze endogene. Ann. Geofis. 8, 1–94 (in Italian).

Penta F (1963) Sulle caratteristiche idrotermologiche dell'isola d'Ischia(Napoli). Rendiconti dell'Accademia dei Lincei, 34, 1-8 (in Italian).

Penta F, Conforto B (1951) Sulle trivellazioni in aree idrotermali per ricerche di vapore. L" ingegnere, Riv. Tecn. Mens. Ass. Naz. Ingg. Archt. It., Milano, 3, 12 (in Italian).

Pollard, D D, & Johnson, A M (1973). Mechanics of growth of some laccolithic intrusions in the Henry Mountains, Utah, II: bending and failure of overburden layers and sill formation. Tectonophysics, 18(3-4), 311-354.

Pous J, Heise W, Schnegg P A, Muñoz G, Martí J, & Soriano C (2002) Magnetotelluric study of the Las Canadas caldera (Tenerife, Canary Islands): structural and hydrogeological implications. Earth and Planetary Science Letters, 204(1), 249-263

Ranganayaki R P (1984) An interpretive analysis of magnetotelluric data. Geophysics 49, 1730–1748.

Rao C K, Jones A G, Moorkamp M (2007) The geometry of the Iapetus Suture Zone in central Ireland deduced from a magnetotelluric study. Phys. Earth Planet. Inter., 161, 134–141.

Revil A, Hermitte D. Spangenberg E, &. Cochémé J J (2002) Electrical properties of zeolitized volcaniclastic materials, Journal of Geophysical Research, 107(B8), 2168, 10.1029/2001JB000599

Revil A, Johnson T C, and Finizola A (2010) Three-dimensional resistivity tomography of Vulcan's forge, Vulcano Island, southern Italy, Geophys. Res. Lett., 37, L15308, doi:10.1029/2010GL043983, 2010

Revil A, Le Breton M, Niu Q, Wallin E, Haskins E, and Thomas D M (2017) Induced polarization of volcanic rocks. 1. Surface versus quadrature conductivity, Geophysical Journal International, 208, 826-844 doi: 10.1093/gji/ggw444.

Revil A, Le Breton M, Niu Q, Wallin E. Haskins E. and Thomas D M (2017), Induced polarization of volcanic rocks. 2. Influence of pore size and permeability, Geophysical Journal International, 208, 814-825 doi: 10.1093/gji/ggw382.

Rinaldi A P, Todesco M, Vandemeulebrouck J, Revil A, Bonafede M (2011) Electrical conductivity, ground displacement, gravity changes, and gas flow at Solfatara crater (Campi Flegrei caldera, Italy): Results from numerical modeling, Journal of Volcanology and Geothermal Research, 207 (3-4) 93-105,

Rittmann A (1930) Geologie der Insel Ischia, Z. Vulkanol. Ergbon, (6), pp 1-265

Rosenkjaer G K, Gasperikova E, Newman G A, Arnason K, & Lindsey N J (2015) Comparison of 3D MT inversions for geothermal exploration: Case studies for Krafla and Hengill geothermal systems in Iceland. Geothermics, 57, 258-274.

Saunders S J (2001) The shallow plumbing system of Rabaul caldera: a partially intruded ring fault?. Bulletin of volcanology, 63(6), 406-420.

Sbrana A, Fulignati P, Marianelli P, Boyce A J, Cecchetti A (2009) Exhumation of an active magmatic–hydrothermal system in a resurgent caldera environment: the example of Ischia (Italy). Journal of the Geological Society, 166(6), 1061-1073.

Schön J H (2015) Physical properties of rocks: Fundamentals and principles of petrophysics (Vol. 65). Elsevier.

Schwalenberg K, Rath V, Haak V (2002) Sensitivity studies applied to a two-dimensional resistivity model from the Central Andes. Geophys. J. Int., 150, 673–686.

Sepe V, Atzori S, Ventura G (2007) Subsidence due to crack closure and depressurization of hydrothermal systems: a case study from Mt Epomeo (Ischia Island, Italy). Terra Nova, doi: 10.1111/j.1365-3121.2006.00727.x

Simpson F, Bahr K (2005) Practical magnetotellurics. Cambridge University Press.

Siripunvaraporn, W., Egbert, G., Lenbury, Y., Uyeshima, M., 2005a. Three-dimensional magnetotelluric inversion: data-space method. Phys. Earth Planet. Inter. 150, 3–14.

Siripunvaraporn, W., Egbert, G., & Uyeshima, M. (2005b). Interpretation of two-dimensional magnetotelluric profile data with three-dimensional inversion: synthetic examples. Geophysical Journal International, 160(3), 804-814.

Smith R L, and Bailey R A (1969) Resurgent Cauldrons. U.S.G.S., Washington. The Geological Society of America, Memoir 116: 613-662.

Tait S, Jaupart C, & Vergniolle S (1989) Pressure, gas content and eruption periodicity of a shallow, crystallising magma chamber. Earth and Planetary Science Letters, *92*(1), 107-123.

Tedesco D (1996) Chemical and isotopic investigations of fumarolic gases from Ischia Island (southern Italy); evidences of magmatic and crustal contribution J. Volcanol. Geotherm. Res., 74, pp. 233-242

Tibaldi A, & Vezzoli L (1998) The space problem of caldera resurgence: an example from Ischia Island, Italy. Geologische Rundschau, 87(1), 53-66.

Tibaldi A, Vezzoli L (2004) A new type of volcano flank failure: the resurgent caldera sector collapse, Ischia, Italy. Geophysical Research Letters, 31(14).

Troiano A, Petrillo Z, Di Giuseppe M G, Balasco M, Diaferia I, Di Fiore B, Siniscalchi A, Patella D (2008) About the shallow resistivity structure of Vesuvius volcano. Ann. Geophys. 51, 179–187.

Troiano A, Di Giuseppe M G, Petrillo Z, Patella D (2009) Imaging 2D structures by the CSAMT method. Application to the Pantano di S. Gregorio Magno faulted basin (Southern Italy). J. Geophys. Eng. 6, 120–130.

Troiano A, Di Giuseppe M G, Petrillo Z, Troise C, & De Natale G (2011) Ground deformation at calderas driven by fluid injection: modelling unrest episodes at Campi Flegrei (Italy). Geophysical Journal International, 187(2), 833-847.

Troiano A, Di Giuseppe M G, Patella D, Troise C, De Natale G (2014) Electromagnetic outline of the solfatara–pisciarelli hydrothermal system, campi flegrei (southern italy). Journal of Volcanology and Geothermal Research, 277, 9-21.

Vaselli O, Tassi F, Duarte E, Fernández E, Poreda R, Huertas J (2010) Evolution of fluid geochemistry at the Turrialba volcano (Costa Rica) from 1998 to 2008. Bull Volcan 72(4), 397–410

Vezzoli L (1988) Island of Ischia. Quaderni de 'La Ricerca Scientifica'. Consiglio Nazionale Ricerche Roma 114(10):7–126

Vezzoli L, Principe C, Malfatti J, Arrighi S, Tanguy J C, Le Goff M (2009) Modes and times of caldera resurgence: the< 10 ka evolution of Ischia Caldera, Italy, from high-precision archaeomagnetic dating. Journal of Volcanology and Geothermal Research, 186(3), 305-319

Vozoff K (1991) The magnetotelluric method. In: Nabighian, M.N. (Ed.), Electromagnetic Methods in Applied Geophysics. Application, vol. 2B. Society of Exploration Geophysicists, Tulsa, OK, pp. 641–711.

Weaver J T, Agarwal A K, Lilley F E M (2000) Characterization of the magnetotelluric tensor in terms of its invariants. Geophys. J. Int. 141, 321–336.

Westerman D S, Dini A, Innocenti F, & Rocchi S (2004) Rise and fall of a nested Christmas-tree laccolith complex, Elba Island, Italy. Geological Society, London, Special Publications, 234(1), 195-213.

Yang B, Egbert G D, Kelbert A, & Meqbel N M (2015) Three-dimensional electrical resistivity of the north-central USA from EarthScope long period magnetotelluric data. Earth and Planetary Science Letters, 422, 87-93.